Title

Field Investigation of Advanced Vehicle Reidentification Techniques and Detector Technologies - Phase 1

Authors

Ritchie, Stephen G.
Park, Seri
Oh, Cheol
et al.

Publication Date

2002-03-01

CALIFORNIA PATH PROGRAM
INSTITUTE OF TRANSPORTATION STUDIES
UNIVERSITY OF CALIFORNIA, BERKELEY

Field Investigation of Advanced Vehicle Reidentification Techniques and Detector Technologies – Phase 1

Stephen G. Ritchie, Seri Park, Cheol Oh
University of California, Irvine
Carlos Sun
University of Missouri

California PATH Research Report
UCB-ITS-PRR-2002-15

This work was performed as part of the California PATH Program of the University of California, in cooperation with the State of California Business, Transportation, and Housing Agency, Department of Transportation; and the United States Department of Transportation, Federal Highway Administration.

Final Report for MOU 3008

March 2002

ISSN 1055-1425

California PATH

(Partners for Advanced Transit and Highways)

MOU 3008 Final Report

Field Investigation of Advanced Vehicle Reidentification Techniques and Detector Technologies – Phase 1

Stephen G. Ritchie

Seri Park

Cheol Oh

Carlos Sun*

Institute of Transportation Studies

University of California

Irvine, CA 92697-3600

January, 2002

* Department of Civil and Environmental Engineering, University of Missouri, Columbia, MO 65211

ACKNOWLEDGEMENT

This work was performed as part of the California PATH Program of the University of California, in cooperation with the State of California Business, Transportation and Housing Agency, Department of Transportation; and the United States Department of Transportation, Federal Highway Administration.

The contents of this report reflect the views of the authors who are responsible for the facts and the accuracy of the data presented herein. The contents do not necessarily reflect the official views or policies of the State of California. This report does not constitute a standard, specification, or regulation.

The authors gratefully acknowledge the assistance of Richard Nelson, City of Irvine, Joe Palen, California Department of Transportation; and Steven Hilliard, Inductive Signature Technologies, Inc., in conducting this research.

ABSTRACT

This report presents the results of Phase I of a multi-year research effort on "Field Investigation of Advanced Vehicle Reidentification Techniques and Detector Technologies," and extends previous PATH research by the authors on MOU 336 "Section-Related Measures of Traffic System Performance: Prototype Field Implementation." The focus of this research included the following: significant expansion and enhancement of the ILD-based vehicle reidentification system at a major signalized intersection in Irvine, California to address reidentification of turning vehicles in addition to through vehicles; derivation of improved estimates of fundamental real-time traffic parameters such as speed, volume and vehicle class from single loop detector inductive signatures; development of a new technique for on-line real-time intersection level of service estimation; implementation of a capability for communicating real-time traffic performance data to operators in the City of Irvine Transportation Management Center (TMC); development of a prototype real-time web-site for internet-based access to performance data from the study intersection in Irvine (and other sites in the future); initial testing of a new state-of-the-art detector card (the IST-222, from IST, Inc.); and an initial study of video image processing for future detector data fusion of video and loop signature data. The very encouraging results obtained to date for signalized intersection application of the vehicle reidentification approach suggest that further development and improvement of the vehicle reidentification algorithms for this application would clearly be of value.

Keywords

vehicle signature, inductive loop detector, single loop speed estimation, vehicle classification, vehicle reidentification, signalized intersection, level of service, detector card, data fusion, web-site

EXECUTIVE SUMMARY

California PATH has been leading research in the field of vehicle reidentification. The research reported here builds on and extends previous PATH research by the authors on MOU 336 "Section-Related Measures of Traffic System Performance: Prototype Field Implementation." The research investigates the use of the latest technologies available for traffic detection for collecting more accurate traffic characteristics and traffic data necessary for Intelligent Transportation System (ITS) applications, but which are difficult to obtain. The primary traffic characteristic that this research attempts to measure more accurately is section (or trip) travel time. Travel time has been identified by Caltrans as particularly important for assessing traffic system performance. Travel times are also important because they are inputs to Advanced Traveler Management and Information Systems (ATMIS). The direct measurement of travel times via vehicle reidentification avoids the inaccuracies associated with estimation methods using local or point speeds obtained from point detectors (such as individual loop or other detector stations). In addition, real-time traffic measures such as dynamic origin/destination demand fractions, lane changing, and section densities can be obtained with a vehicle reidentification approach.

This study implemented a real-time traffic surveillance system based on vehicle reidentification technology utilizing vehicle inductive signatures. The developed system has been operated at the intersection of Alton Parkway and Irvine Center Drive in the City of Irvine, California. Although the signalized intersection problem is more complex and challenging than that of a freeway mainline, good real-time traffic performance results have been obtained to date even though signal phase information and some loops were not yet available at the study site. The present system yields valuable real-time traffic information including section travel time, obtained by matching vehicle signatures from upstream and downstream detector stations. In addition, the new real-time level of service procedures developed in this study are readily transferable to other signalized intersections, and the derived LOS criteria for through and turning vehicles are potentially of considerable value to operating agencies interested in real-time congestion monitoring, control, system evaluation, and provision of real-time traveler information.

This study has also shown that the use of inductive vehicle signatures offers significant advantages for single loop estimation of various real-time traffic flow characteristics, including vehicle speeds and vehicle classification. This enables the loop-signature-based vehicle reidentification approach developed by the authors to be widely applied in practice, and not limited by the existence of double loops. The direct estimation of real-time traffic performance data via the developed traffic surveillance system and its availability over the internet will facilitate implementation of a variety of new Advanced Traffic Management and Information System (ATMIS) strategies in California (and elsewhere).

The very encouraging results obtained to date for signalized intersection application of the vehicle reidentification approach suggest that further development and improvement of the vehicle reidentification algorithms for this application would clearly be of value.

TABLE OF CONTENTS

LIST OF FIGURES

LIST OF TABLES

MOU 3008 - Field Investigation of Advanced Vehicle Reidentification Techniques and Detector Technologies – Phase 1

CHAPTER 1 INTRODUCTION

1.1 Background

Research in Intelligent Transportation Systems (ITS) addresses various transportation needs such as efficiency, safety, environmental protection, mobility, and economic viability. Different agencies on different levels try to utilize ITS for improving the transportation system. These agencies range from day-to-day operators and managers of the transportation system to long term designers and planners of the transportation infrastructure. In order to fully exploit the advantages of ITS strategies, accurate and appropriate data need to be collected from the transportation network. Therefore it is vital to develop advanced surveillance systems that can properly support the objectives of ITS.

In the United States and Europe, and particularly in California, there is increasing interest in investigating methods for obtaining trip travel times and other measures, such as density and origin/destination demands, that can be derived from vehicle reidentification systems. By using non-obtrusive and anonymous tracking methods, individual vehicles can be identified and correlated over numerous identification stations, and very specific real time data can be obtained for any vehicle.

California PATH has been leading research in the field of vehicle reidentification. The actual physical sensor for these reidentification systems can be from a variety of different sensor technologies. It can also consist of a combination of technologies. This research builds on and extends previous PATH research by the authors on MOU 336 “Section-Related Measures of Traffic System Performance: Prototype Field Implementation.” The research investigates the use of the latest technologies available for traffic detection for collecting more accurate traffic characteristics and traffic data necessary for ITS applications, but which are difficult to obtain. The primary traffic characteristic that this research attempts to measure more accurately is section (or trip) travel time. Travel time has been identified by Caltrans as particularly important for assessing traffic system performance. Travel times are also important because they are inputs to Advanced Traveler Management and Information Systems (ATMIS). The direct measurement of travel times via vehicle reidentification avoids the inaccuracies associated with estimation methods using local or point speeds obtained from point detectors (such as individual loop or other detector stations). In addition, real-time traffic measures such as dynamic origin/destination demand fractions, lane changing, and section densities can be obtained with a vehicle reidentification approach.

The multi-year research effort, of which Phase I (this report) represents the first year, consists of three major components, based on fully instrumented signalized intersection and freeway sites in the California Advanced Transportation Management Systems Testbed in Southern California.

The first component, which was the focus of this research, involved major expansion of an ILD (inductve loop detector)-based vehicle reidentification system (that was implemented in MOU 336) at a major signalized intersection in Irvine, California, to address reidentification of turning vehicles in addition to through vehicles, develop techniques for on-line real-time intersection level of service estimation, develop a capability for communicating real-time traffic performance data to operators in the City of Irvine Transportation Management Center (TMC), conduct initial testing of a new state-of-the-art detector card (IST-222) from our research partner IST, Inc., and develop a prototype real-time web-site for internet-based access to performance data from the study intersection (and other sites in the future). In addition, a study was undertaken to derive improved estimates of fundamental real-time traffic parameters such as speed, volume and vehicle class from single loop detectors and inductive signatures. Obtaining accurate estimates of vehicle speed from single ILD's (as opposed to dual loop speed traps) enables the vehicle reidentification approach developed by the authors to be widely applied in practice, and not limited by the existence of double loops.

The second component is a field investigation of several emerging and advanced freeway detector technologies developed by the PATH program, including laser and/or video detectors, and a particularly promising new detector named the Embedded Differential Inductance Scanning (EDIS) detector. The EDIS detector has a resolution several orders of magnitude greater than regular ILD's and addresses many of the shortcomings of ILD's. The third component involves an investigation of the fusion of the various advanced detection systems that have been developed by the PATH program (as well as the EDIS detector) for the purpose of vehicle reidentification (or tracking vehicles from one site to another). Until now, each advanced surveillance system has been researched independently and vehicle reidentification has been studied using feature vectors from a single type of detector.

1.2 Report Outline

Chapter 2 presents a study undertaken to derive improved estimates of fundamental real-time traffic parameters such as speed, volume and vehicle class from single loop detectors and inductive signatures. Chapter 3 discusses expansion of the ILD-based vehicle reidentification system at a major signalized intersection in Irvine, California, to address reidentification of turning vehicles in addition to through vehicles. Chapter 4 discusses the development of new techniques for on-line real-time intersection level of service estimation. Chapter 5 presents an overview of a capability developed for communicating real-time traffic performance data to operators in the City of Irvine Transportation Management Center (TMC). Chapter 6 discusses the development of a prototype real-time web-site for internet-based access to performance data from the study intersection in Irvine (and other sites in the future). Chapter 7 reports the results of initial testing of a new state-of-the-art detector card (IST-222) from our research

partner IST, Inc. Chapter 8 discusses an initial study of video image processing for future detector data fusion of video and loop signature data. Finally, Chapter 9 summarizes the conclusions of this research and directions for future research.

CHAPTER 2 REAL-TIME TRAFFIC FLOW MEASUREMENT FROM SINGLE LOOP INDUCTIVE SIGNATURES

2.1 INTRODUCTION

Accurate traffic data acquisition is essential for effective traffic surveillance, which is the backbone of Advanced Transportation Management and Information Systems (ATMIS). Inductive loop detectors (ILDs) are still widely used for traffic data collection in the U.S. and many other countries. Three fundamental traffic parameters, speed, volume and occupancy, are obtainable via single or double (speed-trap) ILDs. Real-time knowledge of such traffic parameters is typically required for use in ATMIS from a single loop detector station, which is the most commonly used. However, vehicle speeds cannot be obtained directly. Hence, the ability to estimate vehicle speeds accurately from single loop detectors is of considerable interest. In addition, operating agencies report that conventional loop detectors are unable to achieve volume count accuracies of more than 90-95%.

As pointed out by Gardner (1), the state of the art of traffic monitoring and surveillance systems can be divided into three areas : sensor technology, data recording and transfer, and data sampling and analysis. Recently, in the field of sensor technology, many devices have been proposed to obtain improved traffic data. These involve the development of radar detectors, video detectors, and automated vehicle identification (AVI) systems, among others. However, many of these new sensors involve high initial costs with reliabilities that are yet to be proven. Moreover, integration with existing sensors, in most cases ILDs, would be more desirable rather than implementing new technologies and disregarding existing investments. From this perspective, new ILD detector card technology which permits collection of vehicle inductive signatures is of great interest.

Accordingly, the main objective of this chapter is to present the derivation of fundamental real-time traffic parameters, focusing particularly on improved vehicle speed estimation, from single loop detectors and inductive signatures. In this respect, the chapter extends the recent work of Sun and Ritchie (2). In addition to improved volume and occupancy estimation, the approach presented also generates real-time vehicle class information.

2.2 BACKGROUND

2.2.1 Vehicle Inductive Signatures

Detector cards used with conventional ILDs are usually bivalent in nature, where the detector card output is either “0” or “1” depending on vehicle presence. However, detector card technology has advanced to the degree where now the inductance change over the loop due to the vehicle’s passage is obtainable. In particular, high scan rate detectors can sample these inductance changes and produce a waveform or “vehicle signature.” Figure 2.1 and

Figure 2.2 present examples of vehicle signatures for different vehicle types for the case of a single loop configuration. While higher scan rates give more accurate vehicle signatures they also generate more data, creating a trade off between the scan rate and the ability to manipulate in real-time the signature data obtained. In this study, the detector scan rate used was 7 milliseconds. In Figures 2.1 and 2.2 the vertical axis is proportional to the change in inductance, and the horizontal axis is time. Vehicle signatures are functions of vehicle speed and vehicle type, and exhibit different features. Therefore, many features can be derived from the vehicle signatures directly or indirectly. Table 2.1 lists some available features from a vehicle signature; these features are illustrated in Figure 2.3. In this study feature vectors are divided into two categories; vehicle specific feature vectors and traffic specific feature vectors. The vehicle feature vectors refer to the ones that are mainly dependent on the vehicle type. Vehicle length is a good example for this category. These features are expected to be invariant, assuming that the same sensor is used with the same installation configuration and under the same driver's behavior. On the other hand, traffic specific features are highly correlated with the traffic conditions such as speed and occupancy. Slew rate, for example, represents the slope value at the point 0.5 of the normalized signature and is shown in Figure 2.3. In this study, the proposed real time traffic measurement system includes a signature processing routine that identifies and extracts feature vectors from regular and problematic signatures. The problematic signatures will be explained in section 2.4.

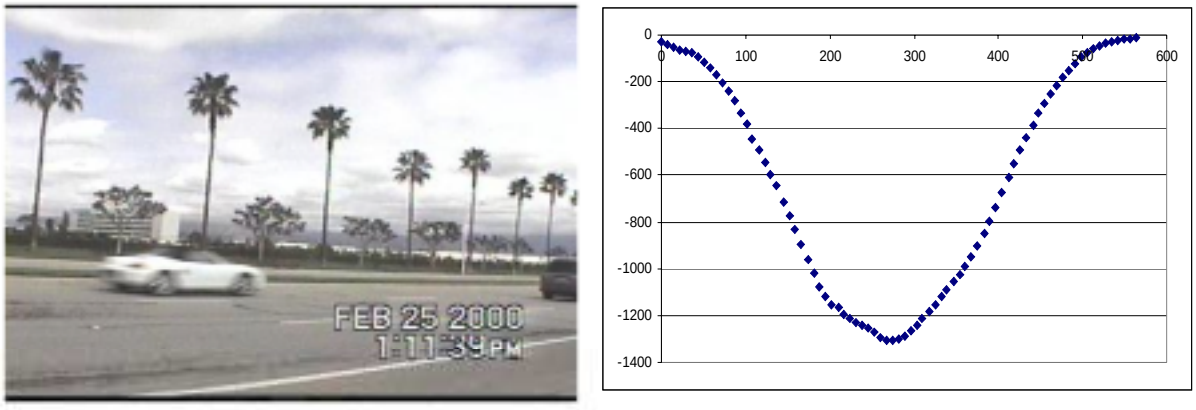

Figure 2.1 Passenger car signature

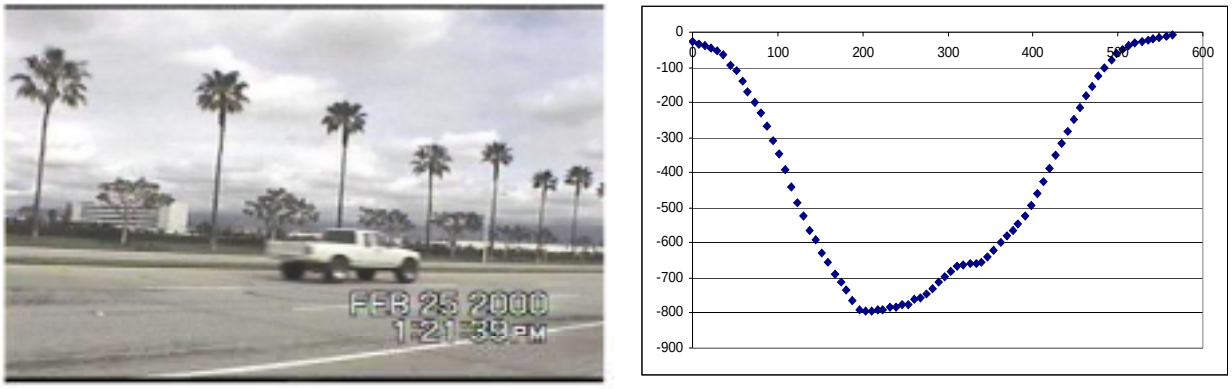

Figure 2.2 Pickup truck signature

Table 2.1 Signature feature vectors (illustrated in Figure 2.3)

Signature Features		**Description**
Vehicle Specific Features	Maximum Magnitude	A
	Magnetic Length	d + e
	Shape Parameter	d / (d+e), related to signature symmetry and skewness
	Signature Area	F
Traffic Specific Features	Slew Rate	c, slope at normalized magnitude of "0.5"
	Duration	b, same as vehicle occupancy

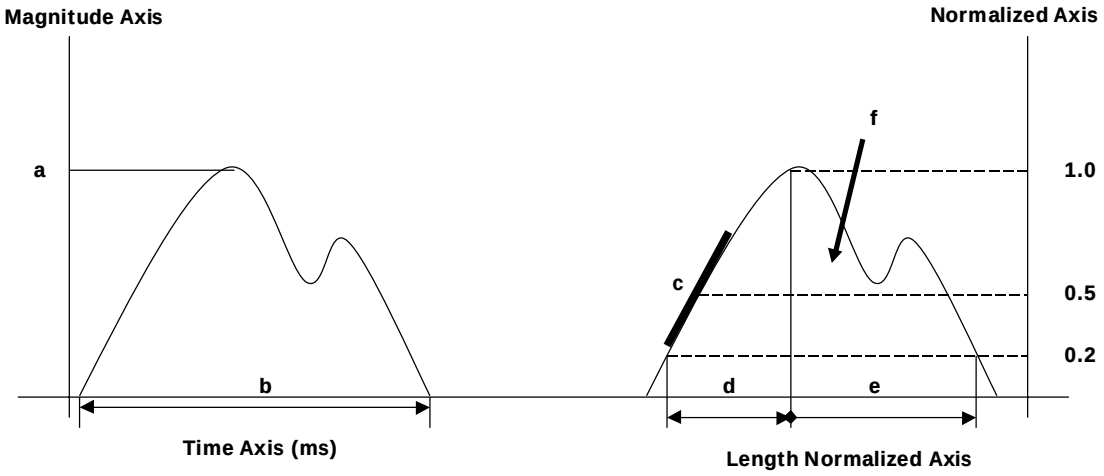

Figure 2.3 Illustration of signature feature vectors (from Table 2.1)

2.2.2 Literature Review

Speed is one of the fundamental traffic variables and at the same time, it can be interpreted as an indicator of transportation system effectiveness. This is because travel time, which is an essential parameter of the transportation system, can be represented as the inverse of speed. It is well known that double ILDs in a speed trap configuration can measure vehicle speeds. However, with the widespread use of single ILDs, a number of researchers have investigated speed estimation from single loops.

By using either a constant or a function to convert loop occupancy into density, the most commonly applied method to obtain speed from a single ILD is based on the relationship between fundamental traffic variables. This approach was first developed by Athol (3) and has been expanded by many researchers such as Mikhalkin et al (4), Courage et al (5), Hall et al (6), Dailey et al (7), Coifman (8), Wang et al (9) and Cherrett et al (10). Approaches that assume a constant vehicle effective length for estimating speed from single loop occupancies are known to produce poor estimates of speed when vehicles of different lengths are present in the traffic stream and when their proportions change over time. Other approaches to speed estimation from a single loop include the use of cusp catastrophe theory (11), statistical methods(12) and video analysis (13).

Recently, Sun and Ritchie (2) proposed a new and straightforward speed estimation technique from single ILD inductive signatures that was based on signal processing and linear regression with very promising initial results. The methodology presented in this chapter extends the work of Sun and Ritchie (2) to develop an expanded and improved system for real-time traffic measurement from single ILDs.

2.2.3 Overview of Methodology and Data

Using advanced loop detector card technology (high speed scanning detector cards that generate vehicle inductive signatures), the proposed system aims to gather accurate and real time traffic measurements such as volume, occupancy, speed, and vehicle classification. In this chapter, estimating vehicle speed is the principal focus. Volume and occupancy are directly derived from processing raw vehicle signatures whereas speed is estimated based on the vehicle signature feature vectors. Vehicle length is obtained based on vehicle speed. By combining vehicle length with existing vehicle signature features, vehicle classification is achieved. Figure 2.4 describes the overall parameter derivation relationship. Field data from a major four - way intersection in the City of Irvine, California was used for system development and performance testing. Details of the dataset can be found in Table 2.2. The data were obtained either from single loops or double loops for several different days (for the double loop data only one loop was used).

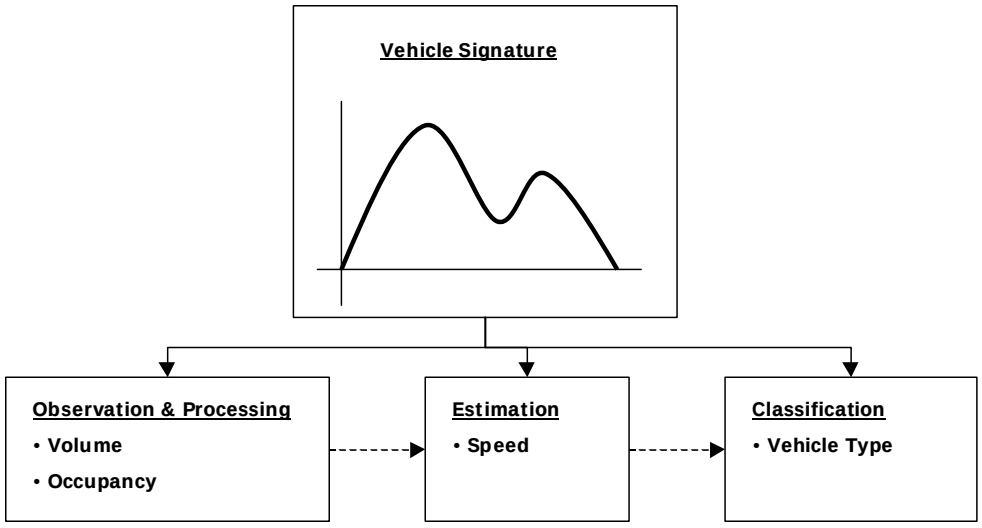

Figure 2.4 Traffic measurements

Table 2.2 Data set description

	Double Loop Vehicles	Single Loop Vehicles
Passenger Car	550	-
Sport Utility Car	150	-
Pickup Truck	190	12
Mini Van	150	-
Van	70	13
One Unit Truck	41	50
Trailer / Vehicle with Boat	45	50
Mini Bus	16	3
Bus	10	-
Total Vehicles	1,222	128

2.3 SPEED ESTIMATION

The study by Sun and Ritchie (2) resulted in a simple linear regression equation between vehicle speed and signature slew rate based on vehicle signatures from single ILDs. For the data used, average speed errors of only about 7 % were obtained from the regression equation. However, when the equation was applied without re-estimation to the data in this study, the results in Table 2.3 for the uncalibrated case were obtained. When the regression parameters were re-estimated, the results for the calibrated case in Table 2.3 were obtained. Interestingly, the results for vehicles with magnetic lengths less than 6 m (mostly passenger cars, but including mini vans, pickup trucks and SUVs) were very good. However, the average speed estimation errors for longer vehicles were quite large. Analysis revealed that the data used by Sun and Ritchie comprised about 94% of vehicles with magnetic lengths less than 6m, possibly explaining the good fit for shorter vehicles and larger errors for longer vehicles. This finding led to a search for an improved approach to estimating single loop vehicle speed. The approach reported in this chapter relies on categorizing vehicles by type (prior to deriving their magnetic length) and estimating separate speed regression equations for each vehicle category.

Table 2.3 Average speed errors for different vehicle lengths using the model of Sun and Ritchie (2)

Magnetic Vehicle Length (ML) Range	Average % error	
	Calibrated case	Uncalibrated case
ML ≤ 6 m	4.19	7.94
6 < ML ≤ 9 m	33.49	30.36
9 < ML ≤ 15 m	33.28	28.36
15 m ≤ ML	16.56	18.38

2.3.1 Features for Speed Estimation

Figure 2.5 shows signatures for the same vehicle (a passenger car) but at different speeds. It is easy to observe signature differences arising from the vehicle's speed. Duration or occupancy has an inverse proportional relationship with speed while slew rate shows a proportional correspondence with speed. Therefore, two traffic specific features, duration and slew rate were chosen as input variables for the new speed estimation models.

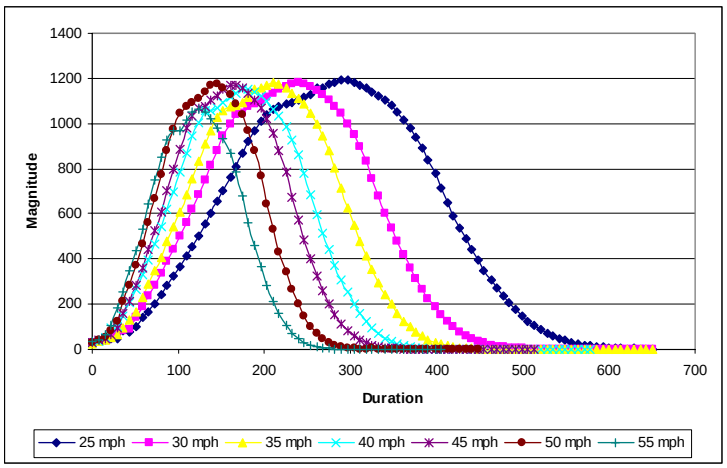

Figure 2.5 Vehicle signatures at different speed for the same vehicle

Figure 2.6 supports the basic concept of the vehicle grouping module, which is discussed in the next section. The two signatures show similar slew rates and durations, but the speeds and vehicle magnetic lengths are quite different. The vehicle grouping module is therefore intended to minimize speed estimation errors originating from incorrect vehicle length assumptions.

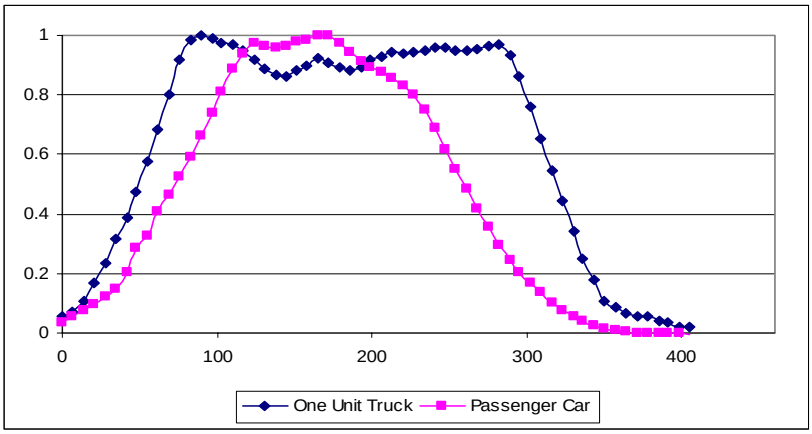

Figure 2.6 Signatures for different vehicles with different speeds, but the same duration

2.3.2 Vehicle Grouping Module

According to Table 2.3, it is clear that the percentage error increases significantly after a vehicle length of 6 m. This suggests that different speed estimation models should be applied and so, prior to this, it is necessary to allocate vehicles to different categories. Six large vehicle classes exist according to Federal Highway Administration (FHWA) vehicle categorizations: passenger cars, motor-cycles, buses, other 2-axle 4-tire vehicles, single-unit 2-axle 6-tire or more trucks, and combination trucks. In this case, other 2-axle 4-tire vehicles include vans, pickup trucks, and sport utility vehicles. Passenger cars and some of the 2-axle 4-tire vehicles show magnetic vehicle lengths less than 6 m. Therefore, based on the FHWA vehicle categorization and extensive data analysis on vehicle magnetic length, four predefined vehicle groups were used. It should be noted that vehicle magnetic lengths can only be derived after speeds are determined. Table 2.4 summarizes four suggested vehicle groups and the corresponding vehicle types as well as the FHWA vehicle category.

Table 2.4 Vehicle grouping

Vehicle Group	Vehicle Type	FHWA Vehicle Category	Magnetic Length (ML)
Group 1	Passenger car, mini van, pickup truck, SUV	Passenger car, other 2-axle 4-tire vehicles	ML <= 6
Group 2	Small bus, van, pickup truck	Other 2-axle 4-tire vehicles	6 < ML <= 9
Group 3	Big bus, one unit truck	Bus, single unit 2-axle 6-tire or more trucks	9 < ML <= 15
Group 4	Trailer, vehicle with boats	Combination trucks	ML > 15

For the purpose of real-time vehicle grouping, a Probabilistic Neural Network (PNN) was applied. The PNN is a neural network implementation of the well established multivariate Bayesian classifier using Parzen estimators to construct the probability density functions (PDFs) of the different classes (14). Application of the PNN is illustrated in Figure 2.7.

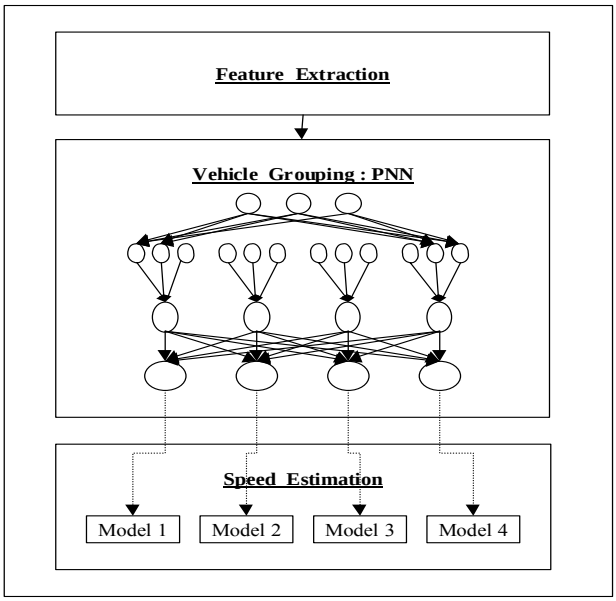

Figure 2.7 Overall PNN procedure

The PNN was trained on a data set of 390 vehicles, and tested with a data set of 195 vehicles. The test results are presented in Table 2.5. Vehicle group 1 shows the highest matching rate (90%) as expected because it had the biggest training dataset. It is also interesting to note the high classification rate (89%) for vehicle group 4 despite its small training sample size of 50 vehicles. By examining the wrongly classified vehicles, it was found that their corresponding magnetic lengths were close to the threshold values of neighboring vehicle groups. For example, in the case of vehicle group 3, six vehicles were misclassified as belonging to vehicle group 2. Five out of those six vehicles showed values around 9.2 m for the vehicle magnetic length, which was very close to the somewhat arbitrarily chosen threshold of 9.0 m between Group 2 and 3 vehicles. This PNN result is therefore reasonable, and could likely be improved with larger training datasets.

Table 2.5 PNN vehicle grouping test result

	Testing Data Results					
	Group 1	Group 2	Group 3	Group 4	Total	Correct Classification Rate(%)
Group 1	45	5	0	0	50	90
Group 2	4	39	7	0	50	78
Group 3	0	6	43	1	50	86
Group 4	0	0	4	41	45	89
Total	49	44	54	42	195	85.8

2.3.3 Statistical Module

Figure 2.6 illustrates the correlation between duration and speed for different vehicle groups. It can be observed that the two variables show a log linear correlation. Therefore, rather than using duration directly, the speed estimation model used log transformed duration. A linear relationship between speed and slew rate was established by Sun et al (2). Accordingly the following linear regression model was proposed for the speed estimation models for individual vehicles in each vehicle group:

$$S_{est\_i} = a + b \cdot sr_i + c \cdot \ln(d_i)$$

where

s_{est_i} : estimated speed of individual vehicle *i*, (m/s)

sr_i : slew rate of individual vehicle *i*

d_i : duration of individual vehicle *i*, milliseconds

a, *b*, *c* : regression parameters

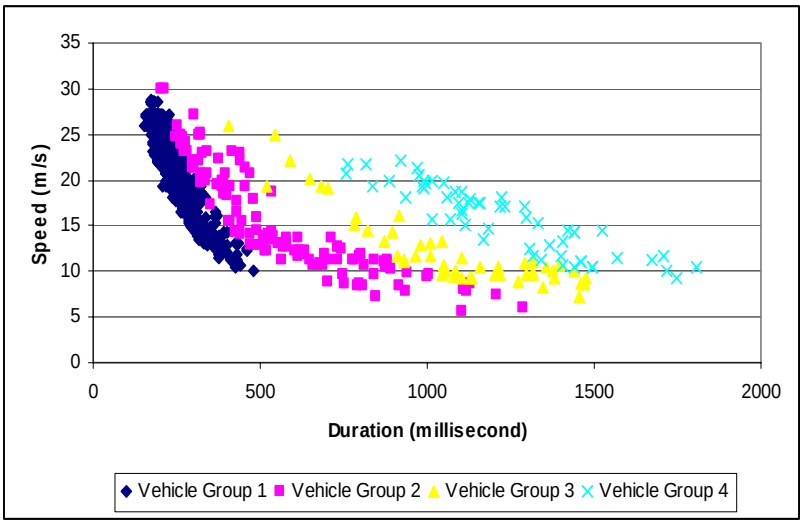

Figure 2.8 Speed and duration

Table 2.6 summarizes the regression results for the proposed statistical speed estimation models for each vehicle group. It should be remembered that errors mentioned in this section solely relate to the regression models. The overall procedure evaluation including the PNN vehicle grouping module is presented in the next section. All the parameters were significant by examining the t-statistics for all models (although in the case of the very long Group 4 vehicles the duration (or loop occupancy) variable was dominant in influencing speed and a new regression was estimated by dropping the slew rate variable). It is interesting to observe that the t-statistic values decrease as vehicle magnetic length increases. The average error in estimated speeds ranged between 5 and 10 %.

Table 2.6 Statistical summary of model results

Vehicle Group	Calibration			Testing		
	Sample Number	Model	Model R^2	Sample Number	Average Error (m/s)	Average Speed Error %
Group 1	800	91.672 + 436.540**SR* – 13.698*ln(*DUR*) (39.393) (13.287) (-36.450)	0.901	200	1.081	5.03
Group 2	65	75.311 + 534.741**SR* – 10.228*ln(*DUR*) (10.874) (4.759) (-10.228)	0.864	61	1.746	9.87
Group 3	35	85.146 + 431.342**SR* – 10.908*ln(*DUR*) (9.191) (3.526) (-8.724)	0.895	16	0.976	6.89
Group 4	45	136.092 – 24.259**SR* – 16.955*ln(*DUR*) (5.261) (-0.094) (-4.975)	0.784	45	1.245	7.14
		133.824 – 16.658*ln(*DUR*) (14.199) (-12.721)	0.784	45	1.236	7.11

Table 2.7 represents the overall results from combining the PNN and regression models for vehicle speed estimation. The results offer a clear improvement over those of Sun and Ritchie (2) with average speed estimation errors of between about 4-15% depending on the vehicle group. The overall average error was less than 10%, which is a very encouraging result. Figure 2.9 presents a scatter diagram of the estimated and actual vehicle speeds. Clearly, most speeds are estimated quite well.

Table 2.7 Overall procedure results

	Sample Number	PNN	Statistical Analysis	
		Correct Classification Rate	Average Error (m/s)	Error (%)
Group 1	50	90	1.05	4.16
Group 2	50	78	1.97	15.17
Group 3	50	86	1.34	9.51
Group 4	45	89	1.70	9.78
		85.8	1.52	9.66

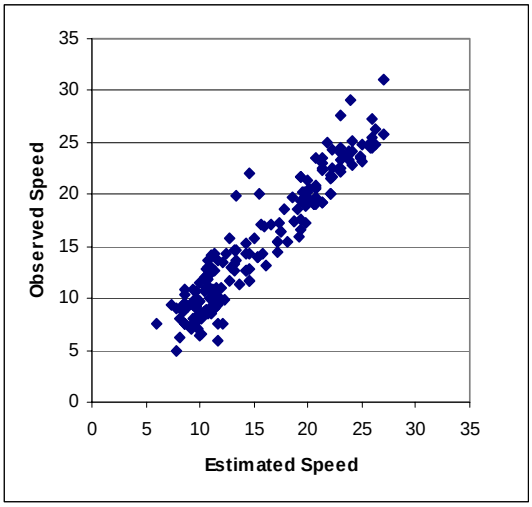

Figure 2.9 Observed speed vs estimated speed

2.4 VEHICLE CLASSIFICATION

Vehicle classification is a process of recognizing vehicle type based on given vehicle characteristics. Accurate vehicle classification has many important applications in transportation. One good example is road maintenance, which is strongly related to the monitoring of heavy vehicles. Incorporating information about vehicle classification in the analysis of environmental impacts is also highly desirable. Improvement of highway safety can also benefit from vehicle classification information, knowing that the severity of traffic accidents is correlated with vehicle types. To summarize, an area-wide assessment of the mix of vehicle classes in traffic is essential for more reliable and accurate traffic analysis and modeling. Therefore, since the 1970's, considerable research has been conducted in this field and new detector technologies have contributed to the enhancement of vehicle classification performance.

In this section, three different neural network (NN) architectures are presented for vehicle classification: backpropagation neural network (BNN), probabilistic neural network (PNN), and self-organizing map (SOM). While the PNN described in the previous section performed well in allocating vehicles to one of four groups or classes, the neural nets described in this section utilize seven different vehicle types for classification purposes. Including vehicle length, which is the most important parameter for vehicle classification, four vehicle specific feature vectors were used as input. Figure 2.10 shows the overall architecture of the BNN and SOM models. The same dataset as for speed estimation was used for NN performance evaluation. The vehicle classification results are presented in Table 2.8, and show that the best overall performance of 82.6% correct classification was obtained from the BNN model.

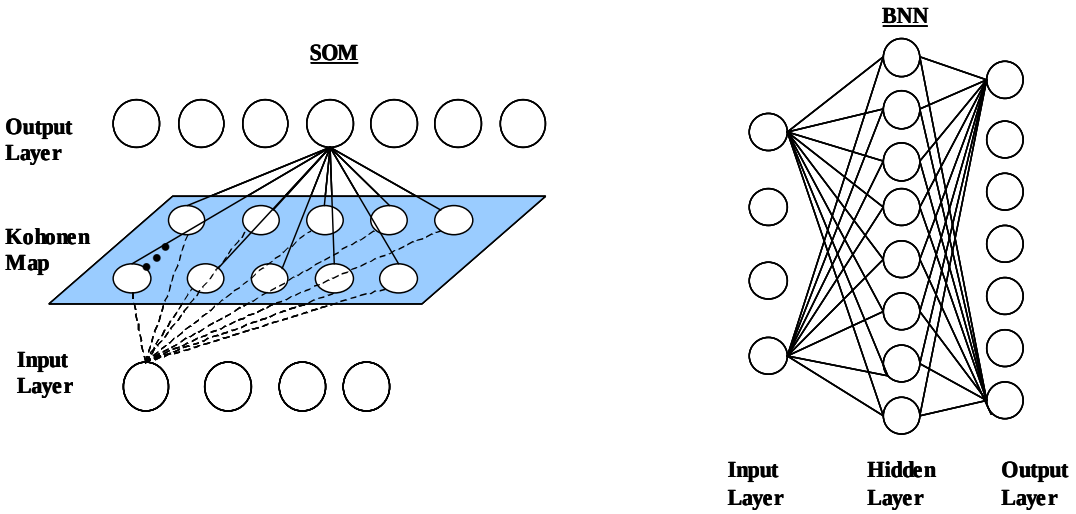

Figure 2.10 Neural network architecture

Table 2.8 Vehicle classification results

Vehicle Type	Training Dataset	Testing Dataset	Correct Classification (Test Dataset) %		
			BNN	PNN	SOM
Passenger car, minivan	100	70	88.6	92.9	90.0
Sport utility vehicle	80	70	74.3	70.0	71.4
Van, minibus	62	40	75.0	65.0	72.5
Pickup truck	100	70	75.7	71.4	64.3
One unit truck	50	41	85.4	80.5	80.5
Trailer / vehicle with boat	50	45	100.0	100.0	100.0
Bus	6	4	100.0	100.0	100.0
Total	448	340	82.6	80.3	78.8

2.5 VOLUME AND OCCUPANCY

ILD volume counts are usually acceptable and reasonable under light traffic conditions unless the ILD is defective. However, with bivalent detector cards tailgating vehicles may be counted as one vehicle, and vehicles with trailers as two vehicles. This results in an incorrect volume count. Figures 2.11 and 2.12 show the signatures obtained for tailgating vehicles and a vehicle towing a boat, respectively. These signatures were obtained using high speed

scanning detector cards. We have developed software to preprocess all signatures and to identify "irregular" signatures such as these. As a result, the accuracy of volume counts and loop occupancies can be significantly increased.

In Table 2.9, the counting result and accuracy are presented for a sample dataset. For this analysis, signature data from an arterial in the City of Irvine was used. Motor cycles were not included in the volume count but can always be detected by changing the sensitivity parameters of the detector card. The true count is based on a manual count observed from a video ground truth study while the signature-based count represents the value obtained after processing the vehicle signatures through the proposed system. In this case, the proposed system was able to address three abnormal vehicle signatures and achieve a volume count accuracy of 99.3%.

Table 2.9 Volume count results

True Count	Detector Count	Signature-based Count	System Accuracy
601	594	597	99.3 %

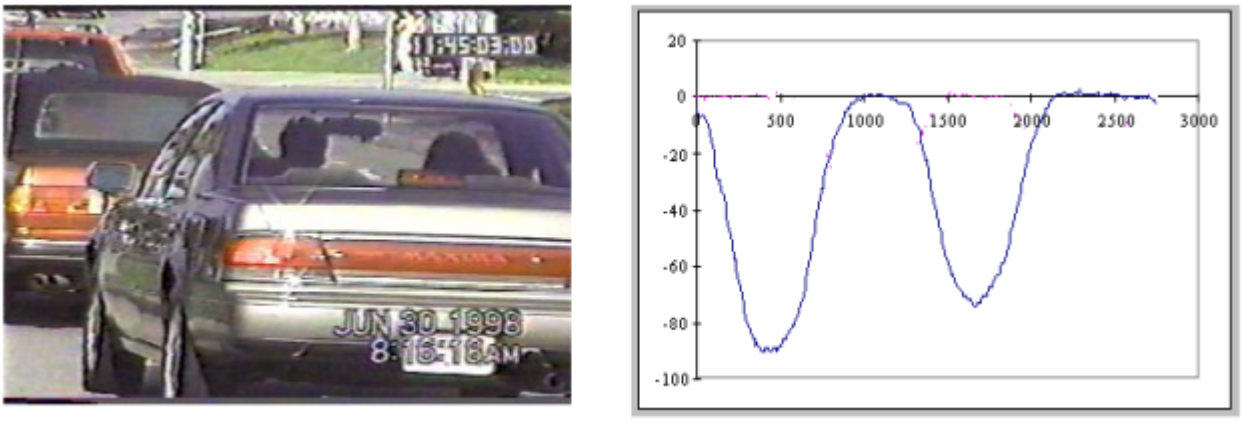

Figure 2.11 Tailgating vehicles signature

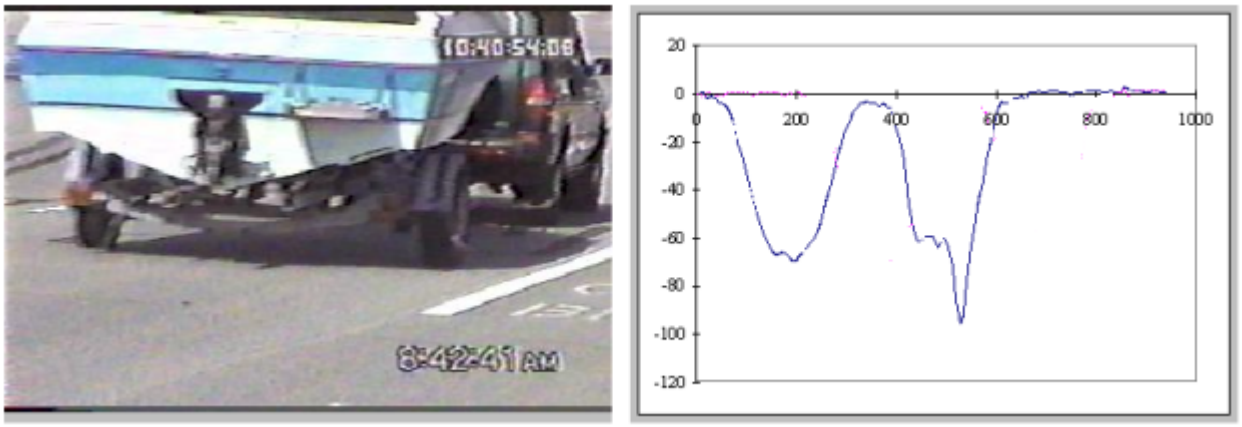

Figure 2.12 Vehicle with boat signature

2.6 CONCLUSION

This chapter has presented a new approach to obtaining real-time flow traffic measurements by using vehicle signatures that are available by integrating existing ILDs with advanced loop detector cards. This approach suggests many advantages. First, by using the current loop infrastructure, it is cost-effective. In addition, unlike other sensors that require a unique vehicle identity, like AVI, this system is non-intrusive and anonymous. Also, advanced sensor technology enables researchers to gather more accurate and reliable traffic data that contributes to more efficient traffic surveillance and control.

In particular, this chapter has demonstrated a new method of individual vehicle speed estimation from single loop detectors. The proposed model estimates individual vehicle speeds in two stages by using models for vehicle grouping and then speed estimation by group. The strength of this study lies in the first stage where the PNN vehicle grouping is accomplished based on the vehicle signature features. Vehicle length influences on speed estimation are considered in this stage as well.

In addition to estimating the individual vehicle speed distribution, the proposed model enables the derivation of useful speed statistics for a specific analysis period. Speed variance, which is a good indicator of traffic flow stability, is also available according to the presented estimation method. Moreover, vehicle classification information yields the composition of vehicle types on the road. This information is an essential requirement for a more accurate analysis of road maintenance and air pollution.

2.7 REFERENCES

1. Gardner, M.P. Highway Traffic Monitoring. Transportation Research Board. *Transportation in the New Millennium*, 2000, pp 5.
2. Sun, C., and Ritchie, S. G. Individual Vehicle Speed Estimation Using Single Loop Inductive Waveforms. *Journal of Transportation Engineering*, 1999, pp 531- 538
3. Athol, P. Interdependence of Certain Operational Characteristics Within a Moving Traffic Stream. *Highway Research Record 72*, HRB, National Research Council, Washington D.C.,1965, pp 58 – 87
4. Mikhalkin, B., Payne, H.J., and Isaksen, L. Estimation of Speed from Presence Detectors. *Highway Research Record 388*, HRB, National Research Council, Washington D.C.,1972, pp 73 – 83
5. Courage, K. G., Bauer, C. S., and Ross, D. W. Operating Parameters for Main – Line Sensors in Freeway Surveillance Systems. *Highway Research Record 602*, HRB, National Research Council, Washington D.C.,1976, pp 19 – 28
6. Hall, F. L., and Persaud, B. N., Evaluation of Speed Estimates Made with Single – Detector Data from Freeway Traffic Management Systems. *Transportation Research Record 1232*, 1989, pp 9 – 16
7. Dailey, D. J., Haselkorn, M. P., and Nihan, N. L. *Improved Estimates of Travel from Real Time Inductance Loop Sensors*. Washington State Department of Transportation, Washington State Transportation Center, University of Washington. 1993
8. Coifman, B. A New Methodology for Smoothing Freeway Loop Detector Data : Introducing to Digital Filtering. *Transportation Research Record 1554*,1996, pp 142 – 152.
9. Wang, Y., and Nihan, N. L. Freeway traffic Speed Estimation with Single Loop Outputs. *Transportation research Record 1727*,2000, pp 120 – 126
10. Cherrett, T., Bell, H., and McDonald, M. Traffic Measurement Parameters from Single Inductive Loop Detectors. *Transportation Research Record 1719*, 2000, pp 112 – 120
11. Pushkar, A., Hall, F. L., and Acha-Daza, J. A. Estimation of Speeds from Single Loop Freeway Flow and Occupancy Data Using Cusp Catastrophe Theory Model. *Transportation Research Record 1457*,1994, pp 149 – 157
12. Dailey, D. J. A statistical Algorithm for Estimating Speed from Single Loop Volume and Occupancy Measurements. *Transportation Research B* Vol 33,1999, pp 313 – 322
13. Dailey, D. J., and Li, L. Algorithm for Estimating Mean Traffic Speed with Uncalibrated Cameras. *Transportation Research Record 1719*, 2000, pp 27 – 32
14. Specht, D.F. Probabilistic Neural Networks and General Regression Neural Networks. In: Chen, C.H. (Ed.), *Fuzzy Logic and Neural Network Handbook*, 1996

CHAPTER 3 ARTERIAL VEHICLE REIDENTIFICATION ALGORITHM ENHANCEMENT

3.1 SITE DESCRIPTION

A real-time traffic surveillance system based on vehicle inductive signatures and vehicle reidentification has been implemented in the City of Irvine, California. The intersection of Alton Parkway and Irvine Center Drive (Alton/ICD) is an eight phase fully actuated intersection where each approach has a set of double loop detectors, referred to as approach detectors. These detectors are about 325 ~ 375 feet upstream from the intersection stop line, except for the eastbound Alton loops which are 800 feet from the intersection. Additionally, there are downstream double loop detectors in each lane right after the intersection; these are referred to as downstream detectors in this study. This brings the total number of loops at the intersection to 48, as shown in Figure 3.1.

Vehicle signature data are extracted in real-time by high-speed scanning loop detector cards. Because of current hardware limitations, vehicle signature data from only one upstream site (Alton Parkway eastbound) and its corresponding three downstreams are collected in real-time.

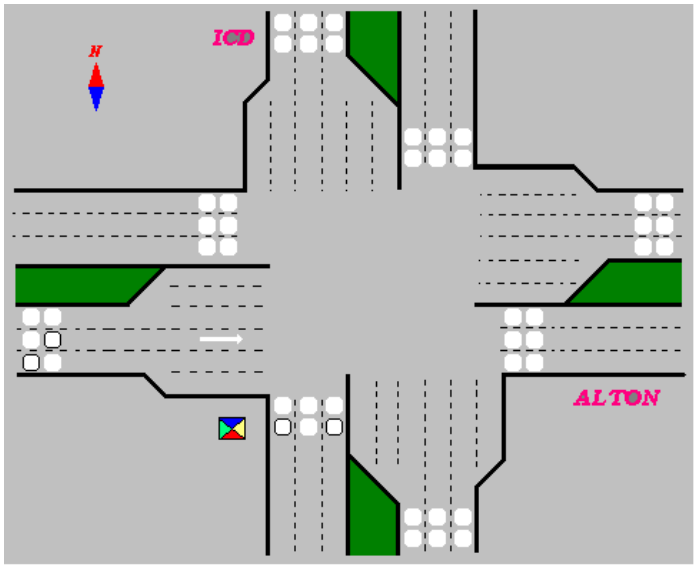

Figure 3.1 Alton/ICD study site

3.2 TURN MOVEMENT FILTERING

The basic idea of vehicle reidentification based on inductive signature is to match a given downstream vehicle signature with an upstream vehicle signature from amongst a set of candidate upstream vehicle signatures. Applying

the concept of the lexicographic method developed by Sun et al. (1) for a freeway application, vehicle reidentification was formulated as a five-level optimization problem. Minimizing mismatches between feature vector pairs denotes the "optimization" on any given objective.

However, unlike the freeway case, an arterial is interrupted by signal control, resulting in highly variable travel times. Each downstream station also has three different upstream stations instead of one, as is typical on a freeway. Turning vehicles also sometimes cross a downstream loop at an angle, or partially cross several loops in adjacent lanes. For these reasons, the optimization is much more challenging than the freeway case. Because of this, an optimization level to filter individual vehicle turning movements was added to identify the upstream origin of each vehicle. This routine of the reidentification process contributes to faster algorithm running times and to improving the matching rate of individual vehicles. The estimation of intersection turning movements is also directly related to the Origin-Destination (OD) matrix at the intersection, and can lead to more effective signal control. Figure 3.2 shows the new framework for arterial vehicle reidentification with embedded turn filtering.

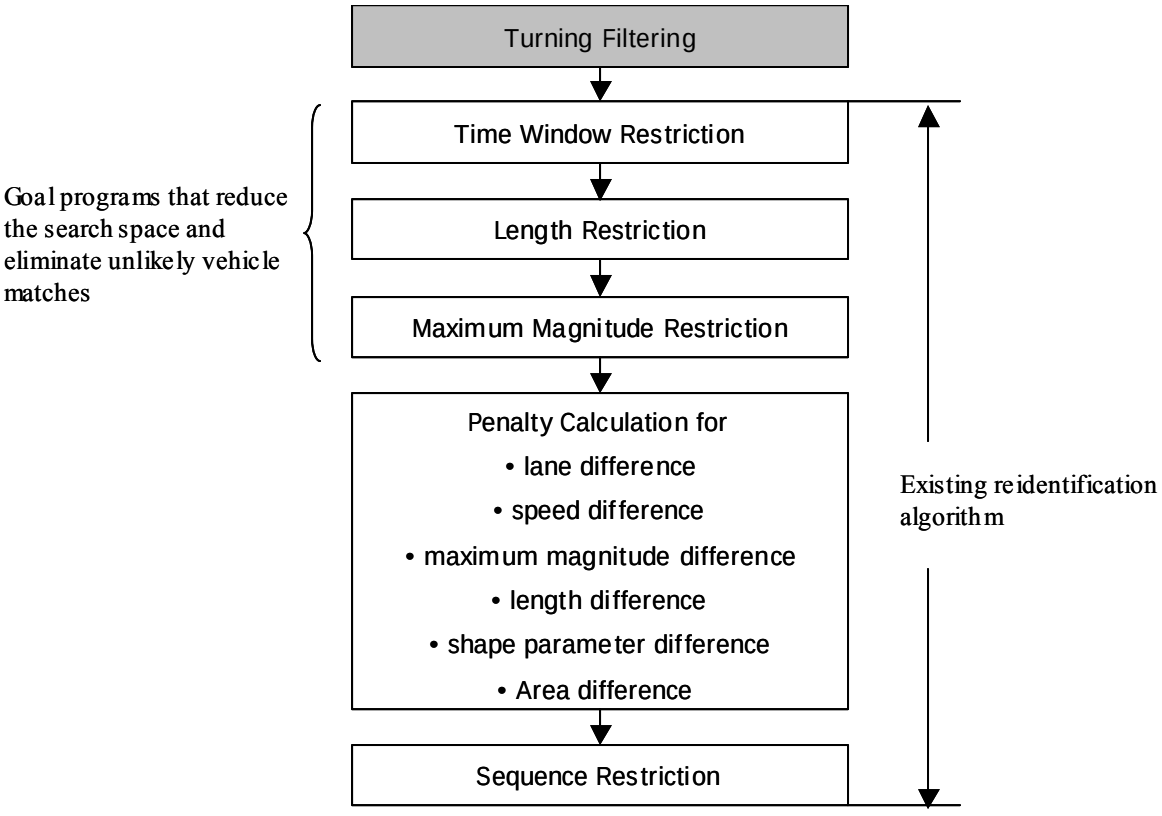

Figure 3.2 Framework for arterial vehicle reidentification algorithm

With the loop detector configuration at the Alton/ICD intersection, as noted above, turning vehicles cross the downstream detectors in different ways. In general, through movements do not change lanes in passing over the downstream detectors. On the other hand, some turning movements do change lanes, and even cross several detectors in adjacent lanes. For example, in Figure 3.3, the right turn movement "C" first hits the front loop in the right most lane and then hits the back loop in the center lane. Moreover, it was observed that turning vehicles often do not pass over the front and back loops completely but hit one or both partially. In Figure 3.3, type "A" represents a partial hit and type "C" represents a lane changing case.

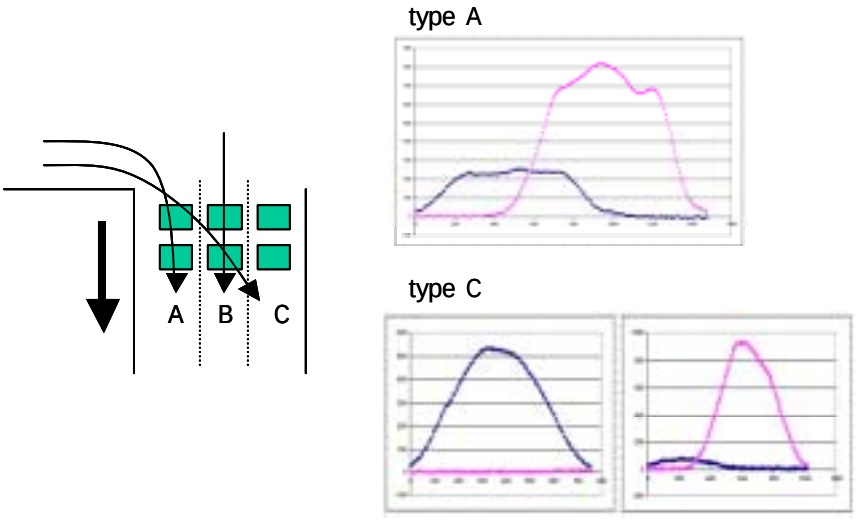

Figure 3.3 Turning vehicle and its characteristics

Figure 3.4 shows the framework for turning filtering based on the observed characteristics of the turning movement behavior. Prior to turning filtering, pre-processing for identifying the appropriate loop array is performed to determine whether a turning vehicle changes lane. If a turning vehicle changes lane, which corresponds type C in Figure 3.3, the algorithm determines the upstream origin based on a combination of the adjacent loop signatures. On the other hand, if a vehicle is determined not to change lane (type A and type B), the algorithm determines the upstream origin based on either a heuristic method or a probabilistic neural network (PNN)-based method.

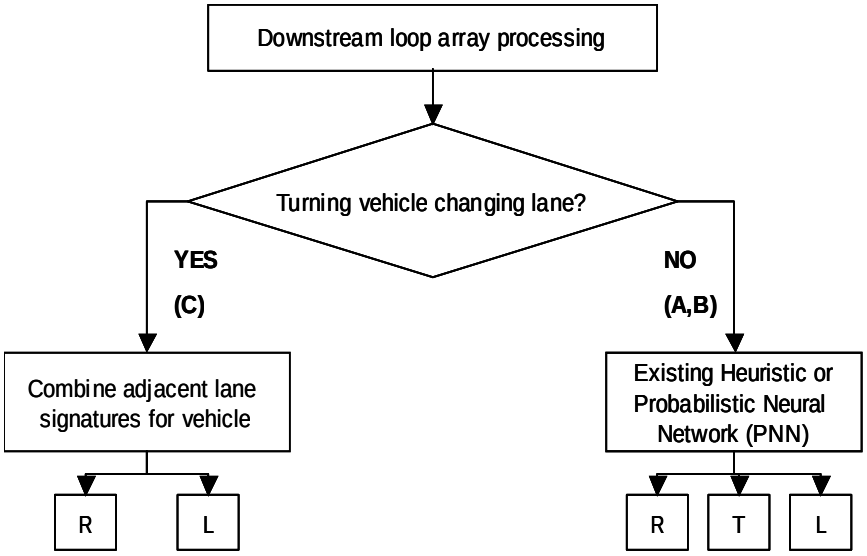

Figure 3.4 Framework for turning movement filtering

3.2.1 Heuristic Discriminant Algorithm

To classify turning movements, heuristic algorithms were developed and embedded in the reidentification system. Three main downstream features, inductive signature maximum magnitude difference between the front and back loops in each lane (max_mag), vehicle speed, and lane information, were used in this algorithm.

As shown in Figure 3.5(a), the speed distributions for each movement have different shapes, which helps to differentiate the movements. The average speed for through movements is higher than for any other movements, and the average speed for right turn vehicles is lower than that of left turn vehicles. It is also identified by Figure 3.5(b) that the range of maximum magnitude difference for turning vehicles is wider than that of through vehicles. These characteristics, obtained by field data analysis, were used to build up a heuristic classification algorithm. The movements are classified using a decision tree approach based on threshold values that minimize misclassification rates. The maximum magnitude is used for the single loop case and the maximum magnitude difference between front and back loops is used for double loop case, as shown in Figure 3.6.

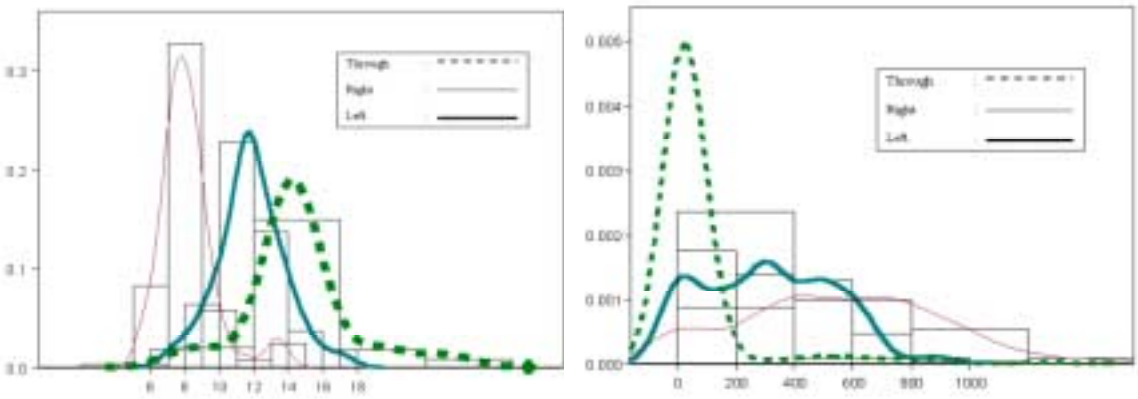

(a) speed (b) maximum magnitude difference

Figure 3.5 Comparison of distributions

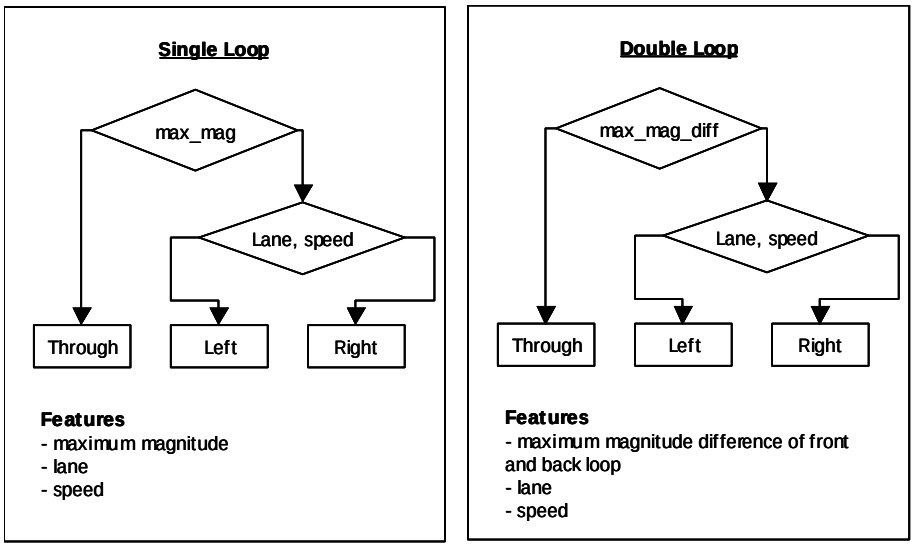

Figure 3.6 Heuristic classification algorithm for turning filtering

3.2.2 Probabilistic Neural Network

The PNN is a neural network implementation of the well established multivariate Bayesian classifier using Parzen estimators to construct the probability density functions (PDFs) of the different classes. Bayesian classifiers were developed in the 1950's, followed by Parzen estimators which were developed to construct the probability density functions required by Bayes theory. Parzen estimators asymptotically approach the true underlying class PDFs as the number of training samples increase. An example of the Parzen estimation of the PDFs is given below for the special case that the multivariate kernel is a product of the univariate kernels. In the case of the Gaussian kernel, the multivariate estimates can be expressed as:

$$f_k(X) = \frac{1}{(2\pi)^{p/2}} \frac{1}{m} \sum_{i=1}^{m} \exp\left[-\frac{(X - X_{ki})^T (X - X_{ki})}{2\sigma^2} \right]$$

k:class, i:pattern number, m:total number of training patterns
X_{ki}:the ith training pattern from category from π_k
σ:smoothing parameter p:the dimentionality of input(feature) space

The PNN consists of four layers as shown in Figure 3.7. The input units are merely distribution units that supply the same input values to all the pattern units. Each pattern unit forms a dot product of the pattern vector X with a weight vector W_i (one examplar pattern i stored as a weight vector W_i) such that $Z_i = X W_i$, and then performs a nonlinear operation on Z_i before outputting its activation level to the summation unit. Instead of the sigmoid activation function commonly used for the Multi Layer Feedforward (MLF) type of neural networks, the nonlinear operation used here is $\exp[(Z_i - 1)/\sigma^2]$. Assuming that both X and W_i are normalized to a unit length, this is equivalent to using $\exp[-\frac{(w_i - X)^T (w_i - X)}{2\sigma^2}]$, which is the same form as the Parzen estimator using a Gaussian kernel. Thus the dot product, which is accomplished naturally in neural interconnections, is followed by the neuron activation function (the exponentiation). Each summation unit sums the outputs from the pattern units that correspond to one of the classes. The output units are three input neurons that produce probabilistic outputs based on Bayesian theory.

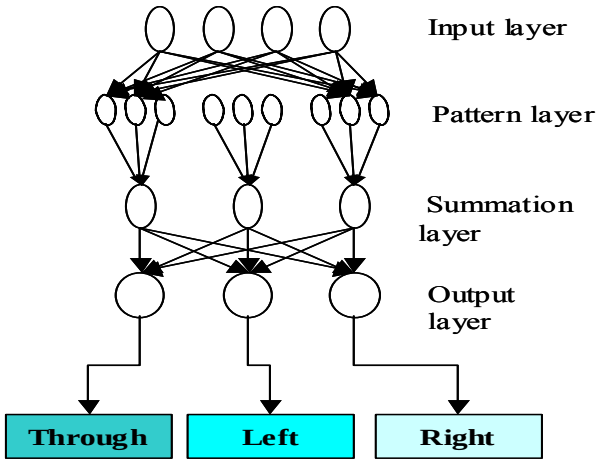

Figure 3.7 Probabilistic neural network (PNN)

The PNN operates entirely in parallel unlike many other neural networks, without the need for feedback from individual neurons to the preceding layer of neurons. The PNN is based on the well-known Bayes theorem, and also the well-known Parzen windows concept, which means the PNN is statistically and theoretically well established with minimal heuristics.

Three PNN inputs were used, drawn from the vehicle signature features discussed in Chapter 2, and based on a Bayesian decision theory study: maximum signature magnitude, slew rate and duration. Signal phase information was not available, but would likely be an extremely valuable additional feature.

3.2.3 Results and Remarks

A data set collected from 09:30 ~ 11:00am on August 16th, 2000 was used to investigate turn filtering algorithm performance. Video ground-truthing was also conducted to identify the true turning movements. The results obtained by the heuristic- and PNN-based filtering algorithms are shown in Table 3.1.

Table 3.1 Turning filtering results

Movements	Classification results	
	Heuristic	PNN
Through	93.6% (279/298)	95% (283/298)
Left	87.5% (7/8)	67% (5/8)
Right	69.3% (79/114)	83% (90/114)
Overall	86.9% (365/420)	90.0% (378/420)

Clearly, the PNN turn filtering algorithm performed slightly better overall. For both algorithms, field data collection and analysis would be required to transfer the turn filtering algorithms to other locations. Use of the PNN based classification algorithm requires modification of the training data. For the heuristic algorithm, the threshold values would need to be modified. Nevertheless, the PNN-based algorithm is recommended for further development because similar efforts are likely needed for transfer of either algorithm. However, the performance of the PNN was slightly better than the heuristic, and the possibility of utilizing the real-time learning capability of the PNN makes it more attractive. The PNN uses the training patterns directly as connection weights, which means off-line retraining is not needed. If TMC operators overwrite newly verified signature feature data onto the training data set, the performance of the PNN will gradually improve.

3.3 OVERALL VEHICLE REIDENTIFICATION MATCHING RESULTS

Two data sets were prepared for testing the performance of the overall vehicle reidentification algorithm. Data were collected on August 16, 2000 during an AM non-peak period from 9:30-11:00am, and on November 16, 2000 during a PM peak hour from 5:00-6:00pm. Data were recorded only for upstream Alton Parkway eastbound and the corresponding three downstream locations. In this application, signal phase information was not available. Signature data were obtained from single loop detectors in lane 2 and 3 of the Alton Parkway westbound approach and in lane 1 and 3 of ICD northbound for the AM non-peak data set, due to 2070 controller hardware limitations. Signature data for ICD southbound in the PM peak data set were collected from single loop detectors in lanes 1 and 3. Tables 3.2 and 3.3 summarize the vehicle reidentification performance for the data sets in terms of correctly matched upstream vehicles for the AM and PM periods, respectively.

Table 3.2 Performance of the overall vehicle reidentification technology (AM data set; PNN-based turn filtering)

		Total Volume		Matching
Upstream (Alton Parkway Eastbound) Lane 1: double loop Lane2,3: single loop		Through	298	
		Left	8	
		Right	114	
		U-turn	2	
		Total	422	
Down-stream	Alton Parkway West bound (all double loop)	1029 ⇒ about 29% from through		52.3% (156/298)
	ICD North bound (Lane2: double, Lane1,3: single)	793 ⇒ about 14% from right turn		33.3% (38/114)
	ICD South bound (all double loop)	581 ⇒ about 1.4% from left turn		25% (2/8)

Table 3.3 Performance of the overall vehicle reidentification technology (PM data set; PNN-based turn filtering)

		Total Volume		Matching
Upstream (Alton Parkway Eastbound) Lane 1: double loop Lane2,3: single loop		Through	438	
		Left	18	
		Right	283	
		U-turn	3	
		Total	742	
Down-stream	Alton Parkway West bound (all double loop)	1285 ⇒ about 34.1% from through		35.8% (157/438)
	ICD North bound (all double loop)	1369 ⇒ about 20.8% from right turn		36.1% (102/283)
	ICD South bound (Lane2: double, Lane1,3: single)	876 ⇒ about 2.1% from left turn		33.3% (6/18)

Considering the complexities involved in this application, and the fact that signal phase information and some loops were not available, the initial results presented in Tables 3.2 and 3.3 are quite good.

3.4 TRAVEL TIME ANALYSIS

The primary characteristic that this research attempts to measure more accurately is section travel time. Travel time has been identified by Caltrans as particularly important traffic parameter for evaluating the performance of dynamic traffic systems. Travel times are also important because they are inputs to Advanced Traveler Management and Information Systems (ATMIS). The direct measurement of travel times via vehicle reidentification avoids the inaccuracies associated with estimation methods using local or point speeds obtained from point detectors such as individual loop or other detector stations.

Arterial traffic flow is interrupted by signal control resulting in highly variable travel times. Therefore, the stability of average travel time is related to the data aggregation period. Several aggregation periods were herefore investigated, as shown in Table 3.4. The average percentage error of travel time between the vehicle reidentification algorithm and ground truth values was determined for different aggregation periods. The travel time analysis was performed only for through and right turning vehicles. The left turning vehicles were not considered because their number was not large enough to be analyzed.

Table 3.4 Results of vehicle reidentification algorithm travel time analysis

Aggregation Period	AM data (average error, %)		PM data (average error, %)	
	Through	Right	Through	Right
Cycle	25.0	27.0	23.9	22.8
1 min	32.3	26.3	31.2	23.0
2 min	20.0	21.4	26.6	15.5
5 min	12.2	11.7	16.7	14.0
10 min	10.3	8.1	12.5	11.6
15 min	8.3	7.7	10.1	9.7

It is apparent that longer aggregation intervals yield more stable traffic data and smaller errors than shorter intervals. However, there exists a trade-off between average error and aggregation interval length, and therefore the real-time nature of the data. One has to consider this trade-off in selecting an aggregation interval for real-time applications.

These results, and those to be presented in Chapter 4 on level of service, show that quite accurate real-time performance data can be obtained based on the vehicle reidentification algorithms described in this chapter. This very encouraging result suggests that further research to develop improved vehicle reidentification algorithms would be of value.

3.5 RELATIONSHIP BETWEEN TURN MOVEMENT FILTERING AND INTERSECTION OD MATRIX

Turning movement estimation is directly related to estimation of the Origin-Destination (OD) matrix at a signalized intersection. Many researchers have tried to estimate reliable intersection approach turning fractions under the assumption that all required information is readily obtained from the real world. The turning filtering algorithm developed in this research potentially enables one to gather accurate turning movement data directly, based on tracking individual vehicles by using vehicle signature analysis.

Since time-varying turning fractions at signalized intersections can be used as valuable information sources in updating dynamic OD matrices for general urban networks, the proposed turning filtering algorithm could not only constitute one of the essential elements for the formulation and estimation of dynamic network ODs, but also contribute to effective real-time adaptive signal control.

3.6 REFERENCES

1. Sun, C., Ritchie, S.G., Tsai, W., and R. Jayakrishnan. Use of Vehicle Signature Analysis and Lexicographic Optimization for Vehicle Reidentification on Freeways. *Transportation Research, Part C*, Vol 7, 1999, pp 167-185

CHAPTER 4 REAL-TIME INDUCTIVE-SIGNATURE-BASED LEVEL OF SERVICE FOR SIGNALIZED INTERSECTIONS

4.1 INTRODUCTION AND RESEARCH BACKGROUND

The U.S. Highway Capacity Manual (HCM) (1) presents a procedure for estimating control delay, which is used to determine signalized intersection Level Of Service (LOS) and to evaluate intersection performance. The HCM is used extensively by traffic engineers. However, it is intended as an off-line decision support tool for planning and design. To meet user requirements of Advanced Traffic Management Systems (ATMS), new LOS criteria are required for real-time intersection analysis. The objective of this phase of the research was to demonstrate a technique for development of such LOS criteria. The study uses a new measure of effectiveness, called Re-identification Delay (RD) derived from analysis of vehicle inductive signatures and reidentification of vehicles traveling through a major signalized intersection in the City of Irvine, California. RD is defined as the difference between the actual time required to traverse vehicle reidentification stations at a signalized intersection and a base travel time such as that calculated from the speed limit. The availability of real-time LOS is of considerable value to operating agencies interested in congestion monitoring, real-time control, incident detection, provision of real-time traveler information, and system evaluation.

LOS is a key concept for evaluating the operational quality of transportation systems. The HCM LOS criteria for traffic signals are stated in terms of the average control delay per vehicle, typically for a 15-min analysis period. With the capability to obtain RD from a vehicle reidentification system, the possibility of obtaining new LOS criteria that can be used for real-time intersection analysis emerges. Two viewpoints can also be considered for the purpose of real-time intersection analysis. Firstly, operating agencies need to obtain real-time traffic conditions in order to control and manage traffic systems. Secondly, drivers or users of the traffic system require high quality and reliable traffic information to decide their route choice in real-time.

Several studies have been performed relating to the derivation of LOS criteria. As expansions of the existing HCM A-F criteria for increasing urban traffic congestion, Cameron (2) and Baumgaertner (3) proposed extending the LOS criteria from A to J and A to I, respectively. Their concern was that longer delay due to increasing congestion was common. Therefore, criteria representing traffic conditions beyond LOS F were proposed by adding extra categories somewhat arbitrarily. Sutaria *et al.* (4) examined user perceptions of LOS based on user-rating data collected at a signalized intersection. More recently, Pecheux *et al.* (5) presented preliminary analyses about how users perceive level of service and how many levels of service are perceived. The result indicated that two or three levels of service were generally perceived. Madanat *et al.* (6) applied an ordered probit model to determine thresholds for each category for transit LOS using bus rider attitudinal data and based on the existing six levels (A-F) in the HCM. With a different view, Ha and Berg (7) developed safety based LOS criteria using conflict opportunity models that were derived for crossing, diverging, and stopping maneuvers associated with left-turn and

rear-end accidents. Saito *et al*, (8) developed a multilayer artificial neural network (ANN) based LOS evaluation model using the same criteria as in the HCM. Their model used delay data from the Highway Capacity Software (HCS) (9). As the authors mentioned, if one has a capability to obtain delay directly in the field, a higher accuracy of LOS can be achieved. From this brief review of existing studies, it appears that no study has attempted to develop real-time LOS criteria.

This chapter is primarily focused on two issues. The first issue is how to determine the threshold values for partitioning different LOS categories. To provide reliable real-time information, the threshold values should be decided such that RDs within the same category represent similar traffic conditions as much as possible. On the other hand, RDs in different LOS categories should also represent dissimilar traffic conditions. The second issue concerns the aggregation interval to use for RD in deriving LOS categories. An investigation of both fixed and cycle-based aggregation intervals is conducted. Several clustering techniques are then employed to derive LOS categories, including K-means, Fuzzy, and Self-Organizing Map (SOM) approaches.

In this chapter, we present new LOS criteria that can be used for providing both operating agencies and drivers with traveler information and for evaluating real-time intersection performance. The chapter discusses a real-time intersection surveillance system, aggregation issues, determination of LOS criteria based on clustering analysis, and our conclusions.

4.2 REAL-TIME INTERSECTION SURVEILLANCE SYSTEM BASED ON VEHICLE REIDENTIFICATION

As described in Chapter 3, a real-time traffic surveillance system based on vehicle inductive signatures and vehicle reidentification was implemented in the City of Irvine, California. The intersection of Alton Parkway and Irvine Center Drive (Alton/ICD) is an eight phase fully actuated intersection where each approach has a set of double loop detectors, referred to as approach detectors. These detectors are about 325 ~ 375 feet upstream from the intersection stop line, except for the eastbound Alton loops which are 800 feet from the intersection. Additionally, there are downstream double loop detectors in each lane right after the intersection; these are referred to as downstream detectors in this study. This brings the total number of loops at the intersection to 48, as shown in Figure 4.1. Some of these loops were pre-existing at the intersection (for an adaptive signal control study) and some were specially installed for this project. In the future, the city is interested in installing single loops upstream on each link for adaptive control purposes. Our ongoing research will seek to utilize existing sensors and detectors rather than specially installed ones, as in this study.

Vehicle signature data were extracted in real-time by high-speed scanning loop detector cards and stored in a dedicated computer at the Irvine Transportation Center (ITC). These data can be accessed at the Irvine Transportation Management Center (TMC) via a Local Area Network (LAN). A new Wide Area Network (WAN) will also enable transmission of data to the University of California, Irvine (UCI). Because of current hardware

limitations, vehicle signature data from only one upstream site (Alton Parkway eastbound) and its corresponding three downstreams were collected in real-time.

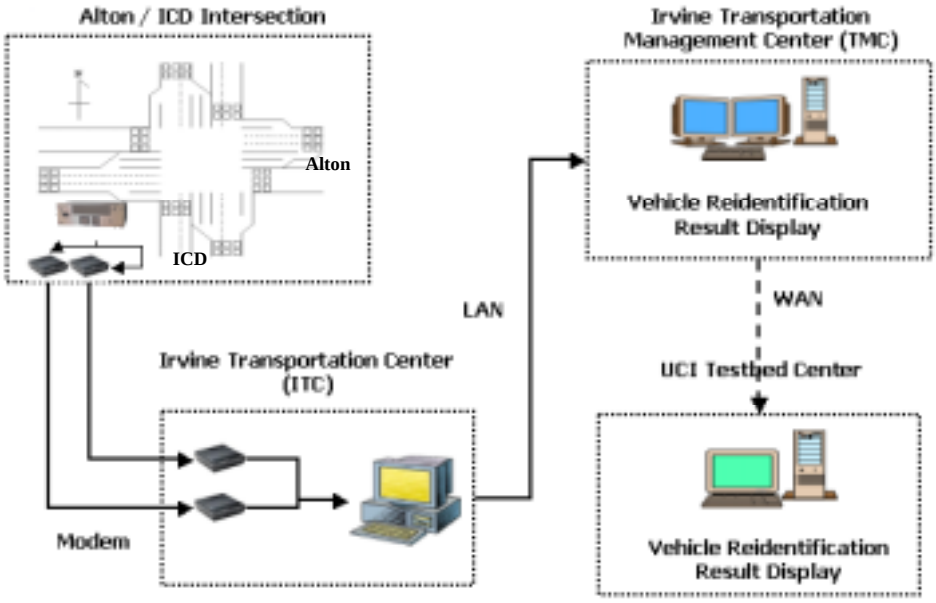

Figure 4.1 Study intersection and data communication

Applying the concept of the lexicographic method developed by Sun et al. (10) for a freeway application, vehicle reidentification was formulated as a five-level optimization problem. Minimizing mismatches between feature vector pairs denotes the "optimization" on any given objective. However, unlike the freeway case, the intersection study site is interrupted by vehicle-actuated signal control, resulting in highly variable travel times. Each downstream station also has three different upstream stations. In this application, signal phase information was not available so, overall, the optimization was much more challenging. Because of this, an optimization level to filter individual vehicle turning movements was added to identify the upstream origin of each vehicle. This routine of the reidentification process contributes to faster algorithm running times and to improving the matching rate of individual vehicles. Intersection turning movement estimation is also directly related to the Origin/Destination (OD) matrix at the intersection.

To classify turning movements, heuristic algorithms were developed (as discussed in Chapter 3) and embedded in the reidentification system. Three main downstream features, inductive signature maximum magnitude difference between the front and back loops in each lane (max_mag), vehicle speed, and lane information, were used in these algorithms. The maximum magnitude of the signature relates to vehicle height since the magnitude is generated according to the vertical distance of the vehicle from the loop. Figure 4.2 shows some characteristics of typical signatures for each movement that were observed at the downstream loop detectors. The vertical axis in each case is proportional to the change in inductance, and the horizontal axis represents time (in milliseconds). Figure 4.3 shows the overall vehicle reidentification algorithm.

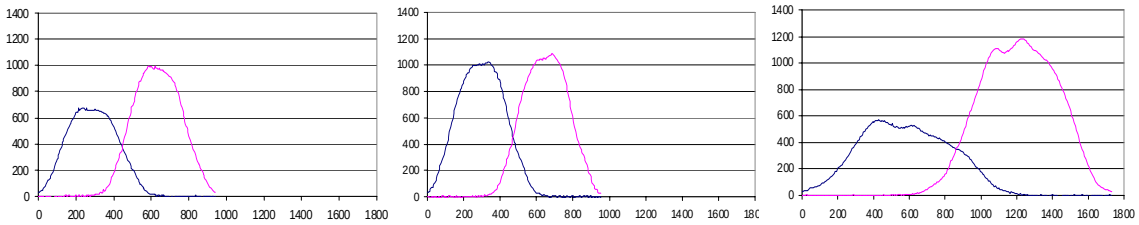

(a) Left-turn signature (b) Through signature (c) Right-turn signature

Figure 4.2 Downstream vehicle signatures for each movement at the study intersection

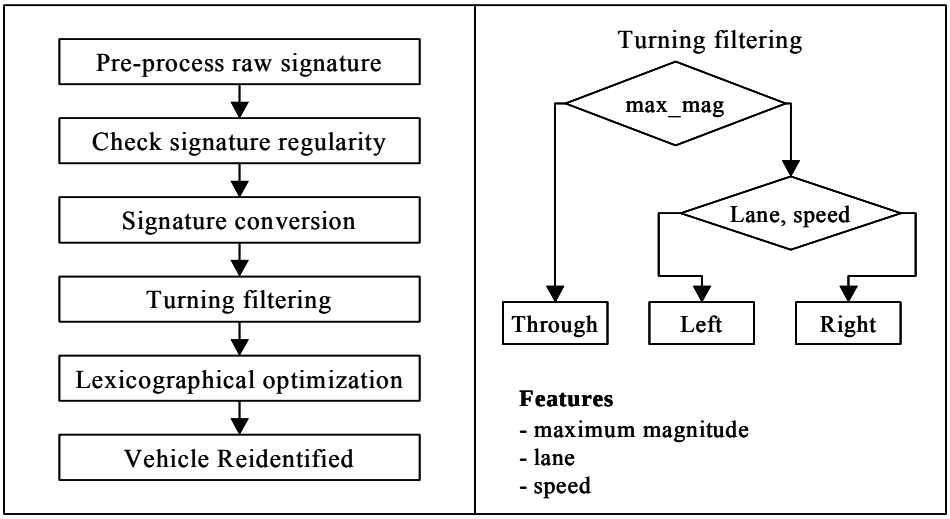

Figure 4.3 Intersection vehicle reidentification flow chart

Data were collected on August 16, 2000 during the AM non-peak hours of 9:30-11:00am. Data were recorded only for upstream Alton Parkway eastbound and the corresponding three downstream locations. The upstream data contained approximately 420 vehicles. Table 4.1 summarizes the vehicle reidentification performance for this data set in terms of correctly matched upstream vehicles. All those vehicles matched by the vehicle reidentification system were used to determine real-time LOS.

Table 4.1 Performance of vehicle reidentification (with heuristic turn filtering)

	Through	Right	Left	Overall
Matching Rate (%)	51.7	32.5	62.5	46.7

A differenece between RD and control delay, which is used as the basis of LOS in the HCM, exists due to the loop configuration of our instrumented intersection. Figure 4.4illustrates the definitions below of RD and control delay with the associated time-distance relationship for a specific vehicle. As identified in Figure 4.4, RD and control delay can be expressed as follows (in order to compute RD we used the speed limit 55mph=V_0).

$$* \text{RD} = (t_6 - t_1) - (\frac{l_6 - l_1}{V_o})$$

$$* \text{Control Delay} = (t_7 - t_2) - (\frac{l_7 - l_2}{V_o})$$

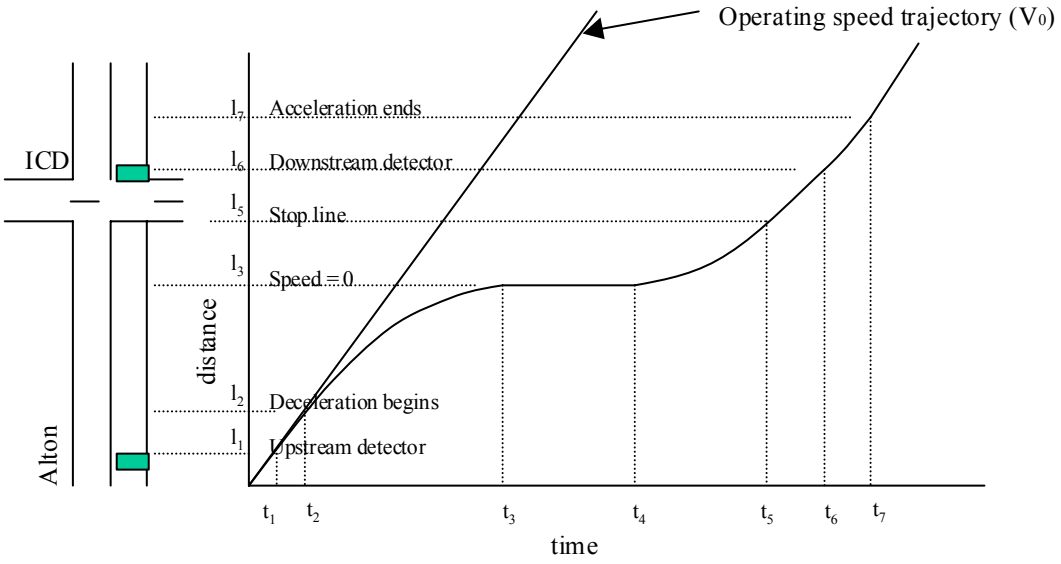

Figure 4.4 Schematic time-distance diagram depicting RD and control delay

4.3 METHODOLOGY FOR DETERMINING LOS CRITERIA

The threshold values used to partition LOS designations should effectively reflect real-time traffic conditions in each category. This partitioning should have the following properties: homogeneity of RD within the same categories, i.e. data that belong to the same category should be as similar as possible, and heterogeneity of RD between categories, i.e. data belonging to different categories should be as different as possible. A solution that can satisfy the above two constraints can be obtained by the formulation of two maximization problems: first to maximize dissimilarity between categories, and second to maximize similarity within categories. Consistent with this, we have applied clustering algorithms to determine the "optimal" number of categories in a given data set. Cluster analysis is different from classification in that no assumptions are made concerning the number of groups. The aim of the cluster analysis is to partition a given set of data or objects into clusters. We investigated K-means clustering, Fuzzy clustering, and an artificial neural network Self-Organizing Map (SOM).

For clustering analysis, the time taken by individual vehicles passing between upstream and downstream detectors corresponds to RD and is an output of our surveillance system. Two time periods representing a range of traffic conditions at the study intersection were selected by field investigation of daily traffic patterns. One data collection period was from 09:30 to 11:20 am, which represents off peak traffic conditions. The other was from 5:00 to 6:00 pm, which represents peak hour traffic conditions. The clustering methodologies were only applied to through and right turn movements due to a lack of left turn data. The collected data are summarized in Table 4.2.

Table 4.2 Collected data for clustering analysis

Data	Through vehicles	Left vehicles	Right vehicles	Total vehicles*
09:30 ~ 11:20	370	9	149	528
17:00 ~ 18:00	438	18	283	739

* at upstream Alton Parkway eastbound station

In addition, RDs, were aggregated into short time intervals, so that the average RD in each period could serve as the basis of the cluster analysis. Two different aggregation methods were investigated: a cycle-length based average (CBA) and a fixed time average (FTA). Because cycle lengths are constantly varying, an on-line algorithm was written to identify the start and end of each cycle. For comparison, a fixed interval of 60 seconds was used for FTA analysis. Figure 4.5 shows a comparison of the two approaches.

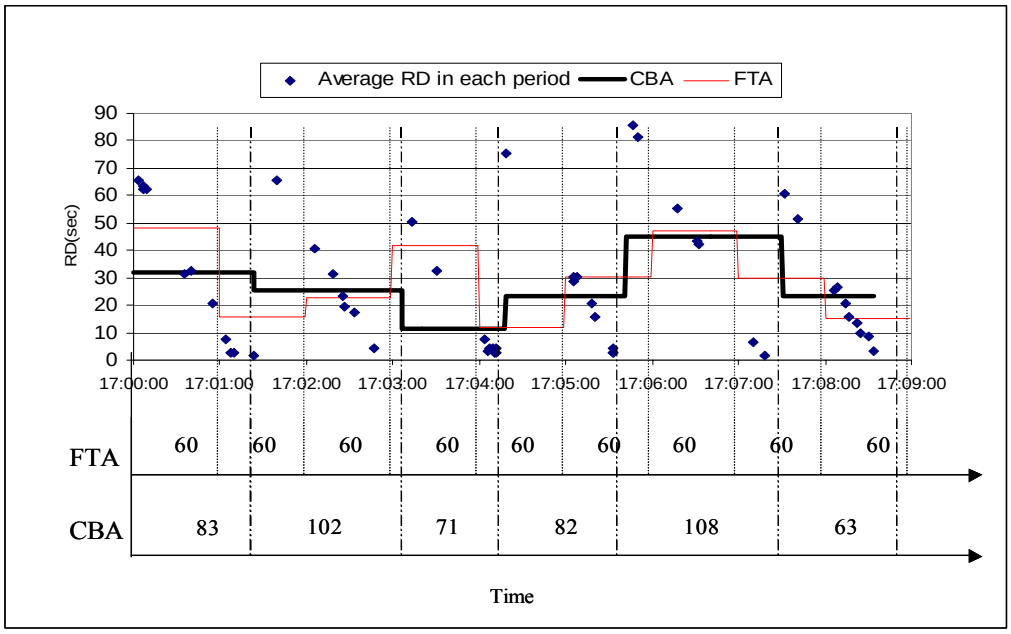

Figure 4.5 Average travel times for different aggregation methods (CBA vs. FTA) for through vehicles

4.3.1 K-means Clustering

K-means clustering is one of the most well known partitioning methods (11). The algorithm computes k representative objects called medoids, which together determine a clustering. The number k of clusters is an argument of the function. Each object is then assigned to the cluster corresponding to the nearest medoid. That is, object i is put into cluster v_i when medoid m_{v_i} is nearer than any other medoid m_w:

$d(i,m_{v_i}) \le d(i,m_w)$ for all $w = 1,....,k$

The k representative objects should minimize the sum of the dissimilarities ($d(i,m)$) of all objects to their nearest medoid:

objective function = $\sum_{i=1}^{n} d(i,m_{v_i})$

4.3.2 Fuzzy Clustering

Unlike conventional crisp clustering, such as K-means where each object of the data set is assigned to exactly one cluster, each observation in fuzzy clustering is given fractional membership in multiple clusters. For each object i and each cluster v, there will be a membership u_{iv} which indicates how strongly object i belongs to cluster v. Memberships have to satisfy the following conditions (12):

$u_{iv} \geq 0$ for all $i = 1,....,n$ and all $v = 1,.....,k$

$\sum_{v=1}^{k} u_{iv} = 1 = 100\%$ for all $i = 1,.....,n$

The memberships are defined through minimization (11) of:

$$\text{objective function} = \sum_{v=1}^{k} \frac{\sum_{i,j=1}^{n} u_{iv}^2 v_{jv}^2 d(i,j)}{2\sum_{j=1}^{n} u_{jv}^2}$$

In this expression, the dissimilarities $d(i,j)$ are known and the memberships u_{iv} are unknown. The minimization is carried out numerically by an iterative algorithm, taking into account the above conditions that memberships need to obey. The result of fuzzy clustering can be shown as crisp clusters by assigning each object i to the cluster v in which it has the highest membership u_{iv}.

4.3.3 Self Organizing Map

The SOM developed by Kohonen is a two-layer neural network that falls into the category of unsupervised learning methodology for clustering and dimension reduction. An advantage of SOM over other clustering algorithms is its ability to visualize high dimensional data using a two-dimensional grid while preserving similarity between data points as much as possible (13). The observations are automatically organized into a meaningful two-dimensional order in which similar ones are closer to each other in the grid than the more dissimilar ones. In this sense the SOM can be regarded as a multivariate clustering algorithm to seek clusters in the data.

Each node of the SOM contains a weight vector, which is equal to the dimension of the feature vectors. Originally, the weight vectors are initialized to random values. During the training, the weight vectors are modified based on the input feature vectors according to the following two steps.

Step1: Search winning node

When each input x is entered into the Kohonen layer, the neurons compute the input intensity $I_j = D(\underline{w}_j, \underline{x})$, where $D(\underline{w}_j, \underline{x})$ is a distance measurement function, in which Euclidean distance is commonly used. After each neuron calculates its I_j, a 'competition' occurs to find the neuron with smallest I_j called the 'winner.'

Step2: Update weight

When the winning neuron c is determined, the weight vectors w are updated according to the following rule:

$$\underline{w}_j^{new} = \begin{cases} \underline{w}_j^{old} + \alpha[\underline{x} - \underline{w}_j^{old}], & j \in N_c \\ \underline{w}_j^{old}, \text{ otherwise} \end{cases}$$

Here N_c is the neighborhood of the winner node c, and α is the learning coefficient. Both are decreasing with time during the training. Steps 1 and 2 are repeated until the map has converged, which may be tested using the average quantization error of the training vectors. As a result of this learning algorithm, the clusters corresponding to characteristic features are formed onto the map automatically. Although SOM identifies a winning neuron based on the same method as employed by traditional competitive learning, it differs from competitive learning in that all neurons within a certain neighborhood of the winning neuron are adjusted instead of adjusting only the winning neurons. After the map has been organized, the clusters can be labeled corresponding to a physical interpretation of the formed clusters.

4.3.4 Clustering Results

To compare the results of each clustering methodology, we used Wilk's lambda (Λ) defined as the ratio of within-groups variance to total variance. A lower Wilk's lambda represents better clustering (14).

$$\Lambda = \frac{|W|}{|T|} = \frac{|W|}{|B+W|}$$

where, W = pooled within-groups variance
B = between groups variance
T = total variance

Average RD based on cycle length (CBA) and fixed time (FTA) intervals was used for clustering. An interval of 60 seconds was used for FTA analysis. Figures 4.6 and 4.7 show the results of clustering for CBA and FTA approaches, respectively.

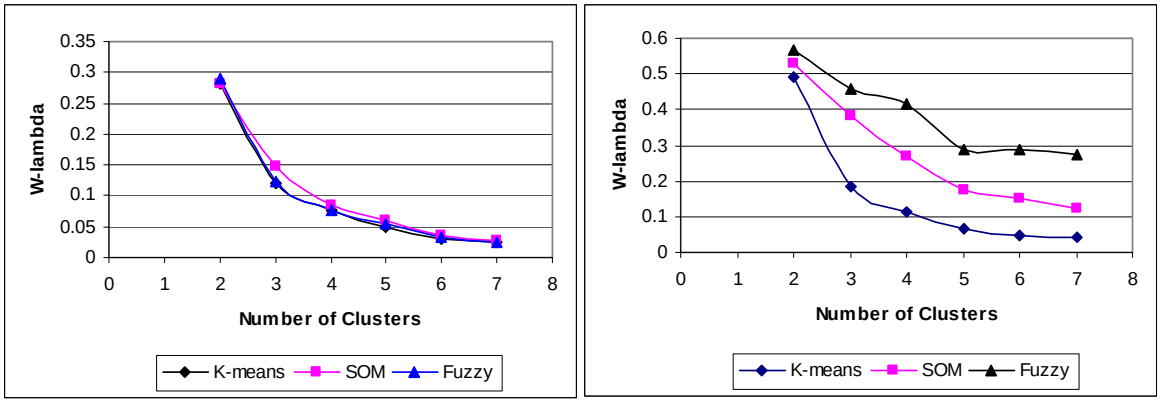

(a) Through vehicles (b) Right vehicles

Figure 4.6 Clustering results based on cycle length based aggregation (CBA)

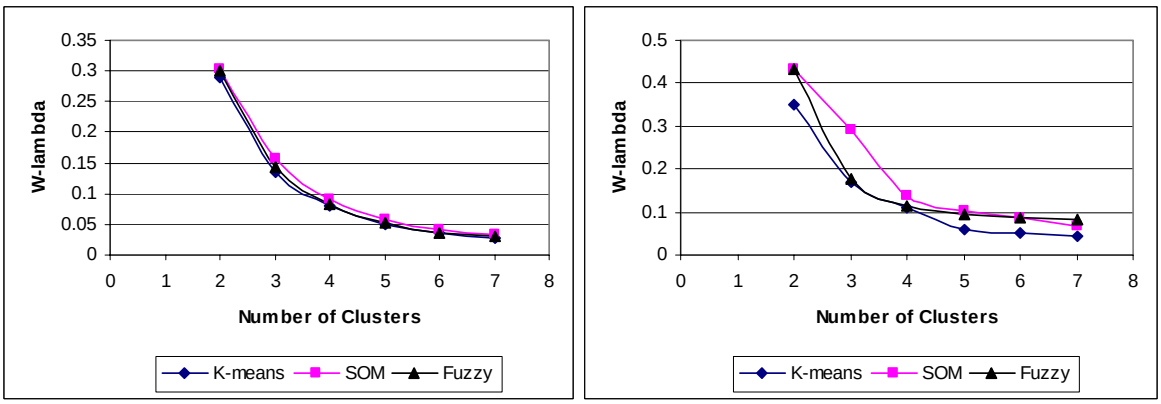

(a) Through vehicles (b) Right vehicles

Figure 4.7 Clustering results based on fixed time aggregation (FTA)

As we can identify in the clustering results, significant marginal improvement due to a decreasing value of Wilk's lambda is not observed after 5 groups, which means the most appropriate number of clusters or LOS categories for the data used is 5. In addition, the overall values of Wilk's lambda from K-means clustering are lower than for the other methods, so the threshold values were determined by K-means clustering. Based on these results, real-time LOS criteria for this signalized intersection can be stated in terms of RD averaged over the cycle length or a fixed 60 seconds interval as shown in Table 4.3. Other longer time intervals could also be used, but if too long, would detract from the "real-time" capabilities of the approach.

Table 4.3 Real-time signalized intersection LOS criteria

LOS Category		LOS criteria (average RD, sec)			
		Through vehicles		Right vehicles	
		CBA	FTA(1min)	CBA	FTA(1min)
I	(Excellent)	≤ 14	≤ 13	≤ 12	≤ 13
II	(Very Good)	> 14 and ≤ 27	> 13 and ≤ 27	> 12 and ≤20	> 13 and ≤ 21
III	(Good)	> 27 and ≤ 41	> 27 and ≤ 45	> 20 and ≤30	> 21 and ≤ 34
IV	(Fair)	> 41 and ≤ 60	> 45 and ≤ 66	> 30 and ≤ 43	> 34 and ≤ 51
V	(Poor)	> 60	> 66	> 43	> 51

For comparative purposes, the six HCM LOS categories based on control delay are presented in Table 4.4. Because the measurement of control delay in real-time is not trivial task, we believe that RD may be more effectively utilized for LOS analysis.

Table 4.4 HCM LOS criteria

Level Of Service	Control Delay per Vehicle (sec)
A	≤ 10
B	>10 and ≤ 20
C	>20 and ≤ 35
D	>35 and ≤ 55
E	>55 and ≤ 80
F	> 80

An analysis of the errors between average RD and actual intersection delay obtained by video ground-truthing for both CBA and FTA aggregation periods yielded the results in Table 4.5. A mean absolute percentage error (MAPE) was used to compute the errors.

$$MAPE = \frac{\sum_{i=1}^{N}\left[\left|\frac{ARD_i - AAD_i}{AAD_i}\right| \times 100\right]}{N}$$

where,

ARD_i = Average Reidentification Delay at time step i

AAD_i = Average Actual Delay at time step i

N = Total number of time step

Table 4.5 Reidentification Delay (RD) errors for different aggregation intervals

Aggregation period	Through vehicles	Right vehicles
Cycle (CBA)	25.0 %	27.0 %
1 min (FTA)	32.3 %	26.3 %

The results in Table 4.5 are dependent on the matching rates achieved by the vehicle reidentification algorithm; as those rates improve so will the errors above. However, even with the initial reidentification performance on which Table 4.5 and the LOS criteria in Table 4.3 are based, the results are believed to be very encouraging.

The authors believe that cycle length may be the shortest appropriate interval to use for data aggregation and LOS purposes, which suggests use of the CBA LOS criteria. In addition to an ability to derive real-time LOS criteria, an advantage of the underlying vehicle reidentification approach is that it permits separate LOS criteria to be developed for through and turning vehicles.

4.4 EXAMPLE REAL-TIME LOS EXAMPLE

To illustrate the application of the results in Table 4.3, consider the actual data and calculated cycle lengths from Figure 4.5. In an on-line situation, the average RD would be calculated at the end of each cycle by the system, and then assigned an appropriate LOS from Table 4.3. In such applications, data aggregation issues could emerge since the stability of delay might be highly variable due to the interruptions of signal control. One could consider the following characteristics regarding the aggregation interval: first of all, dynamic behavior of traffic conditions should be captured by a short aggregation interval. On the other hand, we should be able to provide reliable and stable information, which means, for example, if real-time LOS fluctuates in a short time period, some users might not perceive it as being useful. As one possible solution, a rolling average RD can be used to determine LOS. An aggregation interval that shows a stable change of LOS would be desirable. Various aggregation intervals from 1-cycle to 5-cycles were analyzed. As a result, a 3-cycle rolling average was identified as a reasonable aggregation interval that satisfied above argument. This is illustrated in Table 4.6.

Table 4.6 Real-time LOS analysis

Cycle	Clock Time	Cycle length (sec)	Through Movement				Right-turn Movement			
			1-cycle Average		3-cycle Rolling Average		1-cycle Average		3-cycle Rolling Average	
			RD (sec)	LOS	RD (sec)	LOS	RD (sec)	LOS	RD (sec)	LOS
1	17:00:00 - 17:01:23	83	32.0	III	33.9	III	23.3	III	21.7	III
2	17:01:24 - 17:03:06	102	25.5	II	32.5	III	19.0	II	22.4	III
3	17:03:07 - 17:04:18	71	11.6	I	23.0	III	6.5	I	16.3	II
4	17:04:19 - 17:05:41	82	23.4	II	20.2	II	20.0	II	15.2	II
5	17:05:42 - 17:07:30	108	45.2	IV	26.7	II	28.1	III	18.2	II
6	17:07:31 - 17:08:34	63	23.5	II	30.7	III	13.6	II	20.6	II

The LOS categories determined in Table 4.6 for each cycle could be communicated in real-time to the operating agency's traffic management center, either for direct operator evaluation, or as input to other software applications, such as congestion monitoring.

4.5 CONCLUSIONS

The U.S. Highway Capacity Manual presents a procedure for estimating control delay, which is used to determine Level Of Service and to evaluate intersection performance. The HCM is used extensively by traffic engineers. However, it is intended as an off-line decision support tool for planning and design. To meet the user requirements of Advanced Traffic Management Systems, new LOS criteria are required for real-time intersection analysis. The objective of this research was to demonstrate a technique for development of such LOS criteria. The study used a new measure of effectiveness, called Re-identification Delay (RD) derived from analysis of vehicle inductive signatures and reidentification of vehicles traveling through a major signalized intersection in the City of Irvine, California.

This chapter tackled two main issues regarding real-time LOS criteria. The first was how to determine the threshold values partitioning the LOS categories. To provide reliable real-time traffic information, the threshold values should be decided so that RDs within the same LOS category should represent similar traffic conditions as much as possible. On the other hand, RDs in different LOS categories should also represent dissimilar traffic conditions. The second issue concerned the aggregation interval to use for RD in deriving LOS categories. An investigation of both

fixed and cycle-based aggregation intervals was conducted. Several clustering techniques were then employed to derive LOS categories, including K-means, Fuzzy, and Self-Organizing Map (SOM) approaches. The resulting real-time LOS criteria were presented. The procedures used in this study are readily transferable to other signalized intersections for the derivation of real-time LOS.

In this study, upstream and downstream detectors were used that were not typical of detector configurations found in current practice. Our on-going research is undertaking studies of detector configurations that are able to satisfy the needs of both signal control and vehicle reidentification.

It is believed that the initial techniques for development of real-time LOS criteria developed in this study have provided very encouraging results and offer a valuable tool to operating agencies in support of congestion monitoring, real-time control, and system evaluation. Furthermore, the information could be used for real-time traveler information.

4.6 REFERENCES

1. Special report 209: *Highway Capacity Manual*. TRB, National Research Council, Washington, D.C. 2000
2. Cameron, R. G3F7-An Expanded LOS Gradation System. *ITE Journal*, January, 1996, pp. 40-41
3. Baumgaertner, W.E. Level of Service-Getting Ready for the 21st Century. *ITE Journal*, January, 1996, pp. 36-39
4. Sutaria, T.C., Hayness, J.J. Level-of-Service at Signalized Intersection. In *Transportation Research Record 644*, TRB, National Research Council, Washington, D.C. 1977, pp. 107-113
5. Pecheux, K.K., Pietrucha, M.T., and Jovanis, P.P. User Perception of Level of Service at Signalized Intersections, In *Proceedings, 79th Annual Meeting of the Transportation Research Board*, Washington, D.C. 2000
6. Madanat, S.M., Cassidy, M. J., and Ibrahim W.W. Methodology for Determining Level of Service Categories Using Attitudinal Data. In *Transportation Research Record 1457*, TRB, National Research Council, Washington, D.C., 1994, pp. 59-62
7. Ha, Tae-jun, and Berg W.D. Development of Safety-Based Level-of-Service Criteria for Isolated Signalized intersections In *Transportation Research Record 1484*, TRB, National Research Council, Washington, D.C., 1995, pp. 98-104
8. Saito, Mitsuru and Fan, J. Multilayer Artificial Neural Networks for Level-of-Service Analysis of Signalized Intersection. In *Transportation Research Record 1678*, TRB, National Research Council, Washington, D.C., 1999, pp. 216-224
9. *Highway Capacity Software*. FHWA, U.S. Department of Transportation, 1994

10. Sun, C., Ritchie, S.G., Tsai, W., and R. Jayakrishnan. Use of Vehicle Signature Analysis and Lexicographic Optimization for Vehicle Reidentification on Freeways. *Transportation Research, Part C*, Vol 7, 1999, pp 167-185
11. Kaufman, L. and Rousseeuw, P.J. *Finding Groups in Data: An Introduction to Cluster Analysis*. Wiley, New York. 1990
12. Höppner, F., Klawonn, F., Kruse, R., and Runkler, T. *Fuzzy Cluster Ananlysis: Methods for Classification, Data Analysis and Image Processing*. John Wiley & Sons, LTD, England, 1999
13. Kohonen, T. *Self-Organizing Maps*. Springer, Berlin, 2001
14. Johnson, R.A., and D.W. Wichern. *Applied Multivariate Statistical Analysis*. Prentice-Hall, Englewood Cliffs, NJ, 1992

CHAPTER 5 OVERVIEW OF ON-LINE TRAFFIC MANAGEMENT CENTER IMPLEMENTATION

5.1 INTRODUCTION

The design and implementation of an on-line vehicle reidentification system for the Alton Parkway and Irvine Center Drive intersection is summarized in this chapter. This includes the data flow from the field to the Irvine Transportation Center (ITC) and to the Irvine Transportation Management Center (TMC), the automatic and daily archiving of the reidentified data, and the graphical user interface (GUI) for the vehicle reidentification system.

5.2 GRAPHICAL USER INTERFACE (GUI)

A GUI provides a user friendly environment for the system operation. Extensive work was dedicated to GUI development and implementation, as summarized in the following paragraphs.

Figure 5.1 shows the initial window of the GUI. The selection of either off-line or on-line reidentification operation is determined in the first step. Also, the existence of available signature data from each station should be taken into account, along with desired display options, as shown in Figure 5.2. All those selections were coded to be user friendly by prompting dialogue boxes at each step.

The main window while running the reidentification algorithm is described in Figure 5.3. The two sub-windows at the right side of the screen represent the most recent raw vehicle signature at the upstream and downstream station. The horizontal axis indicates time in milliseconds, and the vertical axis shows the raw signature magnitude. Normalized and reidentified vehicle signature pairs are shown in the lower left quadrant of the screen. Vehicle lengths are expressed in meters on the horizontal axis of this sub-window. Users can easily note the matched vehicle signature pair through this sub-window.

Users can also specify the data display start time as well as updating and analysis intervals, as shown in Figure 5.4.

5.3 ON-LINE IMPLEMENTATION

The existing off-line reidentification algorithm was enhanced and modified for on-line operation. A description of the vehicle signature data flow follows. Vehicle signature data are collected and packed on-site through the 2070 controller using advanced detector cards. This data are then transmitted to a remote and dedicated PC at the ITC, via modems. Vehicle reidentification is accomplished on this computer whenever a vehicle is detected at each downstream station. The reidentified data are automatically stored by creating a daily directory for data archiving. The local area network (LAN) connection of the City of Irvine enables the TMC operators to control and manage the reidentification system remotely. Figure 5.5 illustrates this architecture and the flow of the signature and

reidentified data. As indicated in this figure, the wide area network (WAN) between the City of Irvine and our labs at the University of California, Irvine will provide future access to the on-line system operation and historical data. Figure 5.6 shows the on-line vehicle reidentification system workstation at the City of Irvine TMC.

A more detailed description of the reidentification algorithm architecture is found on Figure 5.7. The algorithm is divided into three main routines, or so-called threads. The Recv thread receives field vehicle signature data and sends it to the LogSig thread that processes and stores the raw signature data. Vehicle reidentification is then performed by the Reid thread. Because of the 2070 controller limitations, some single loop configurations were used at the Alton Parkway upstream station and Irvine Center Drive downstream station. This explains the detector number differences in Figure 5.3.

As discussed in the next chapter, subsequent efforts have been devoted to developing a more accessible web-based means of providing real-time traffic performance data to multiple users, including traffic management center operators.

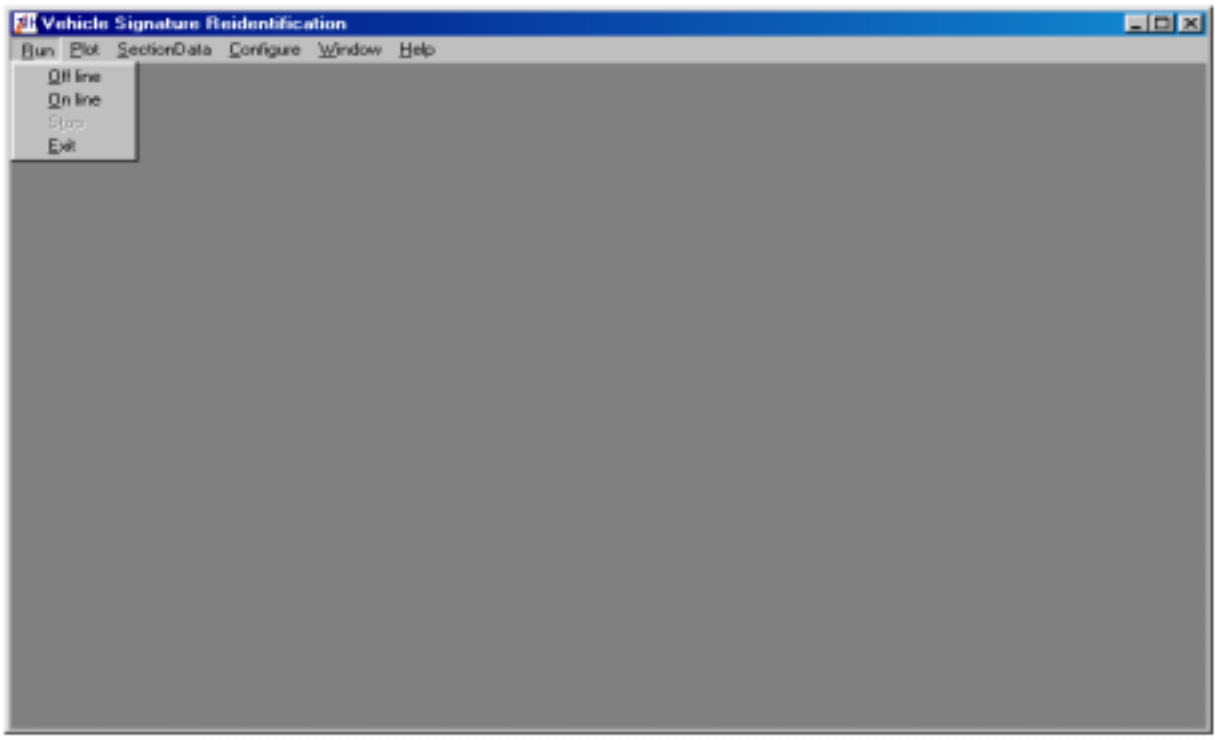

Figure 5.1 Initial window

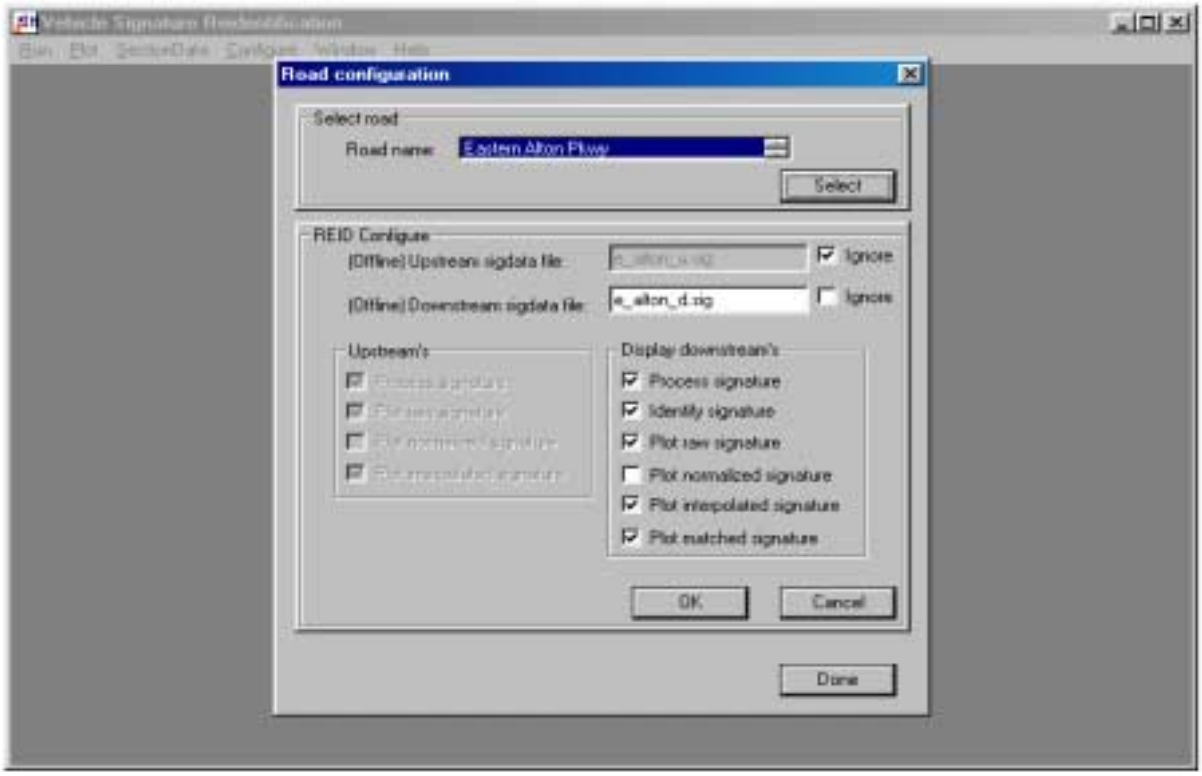

Figure 5.2 Road configuration window

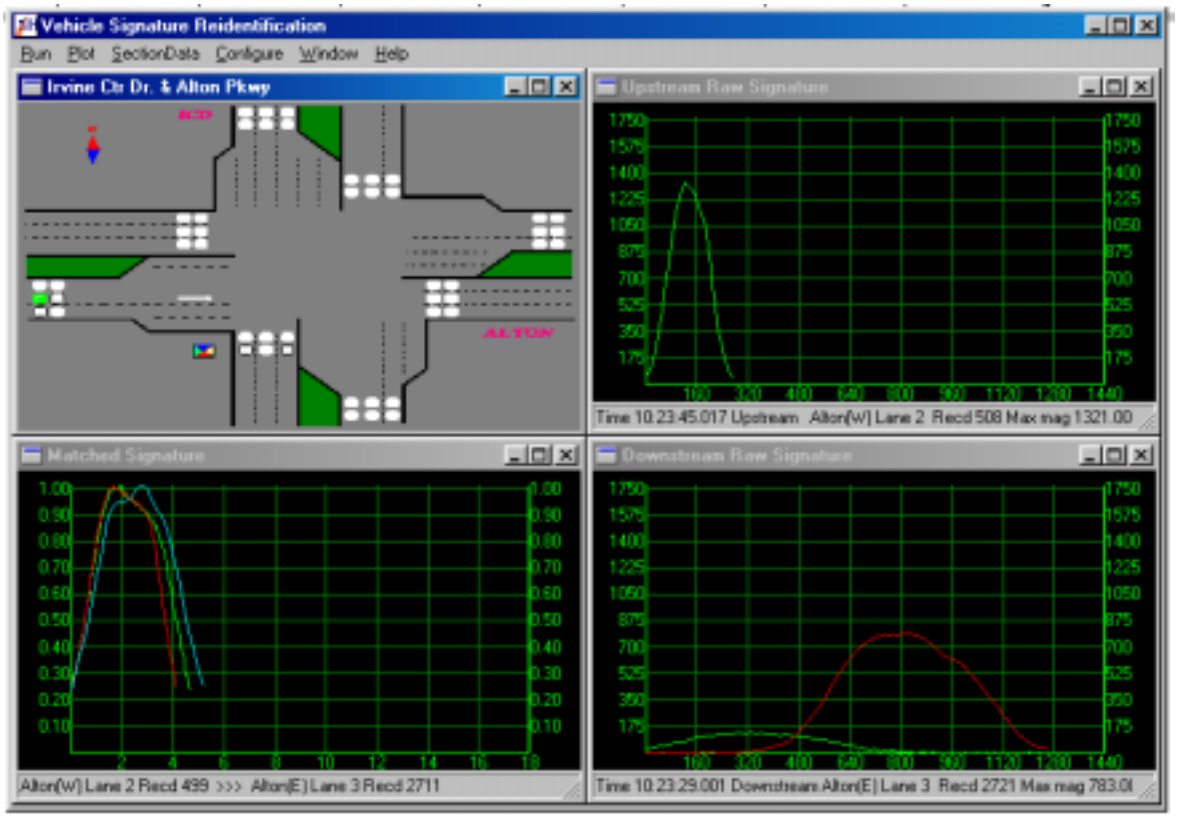

Figure 5.3 Reidentification main window

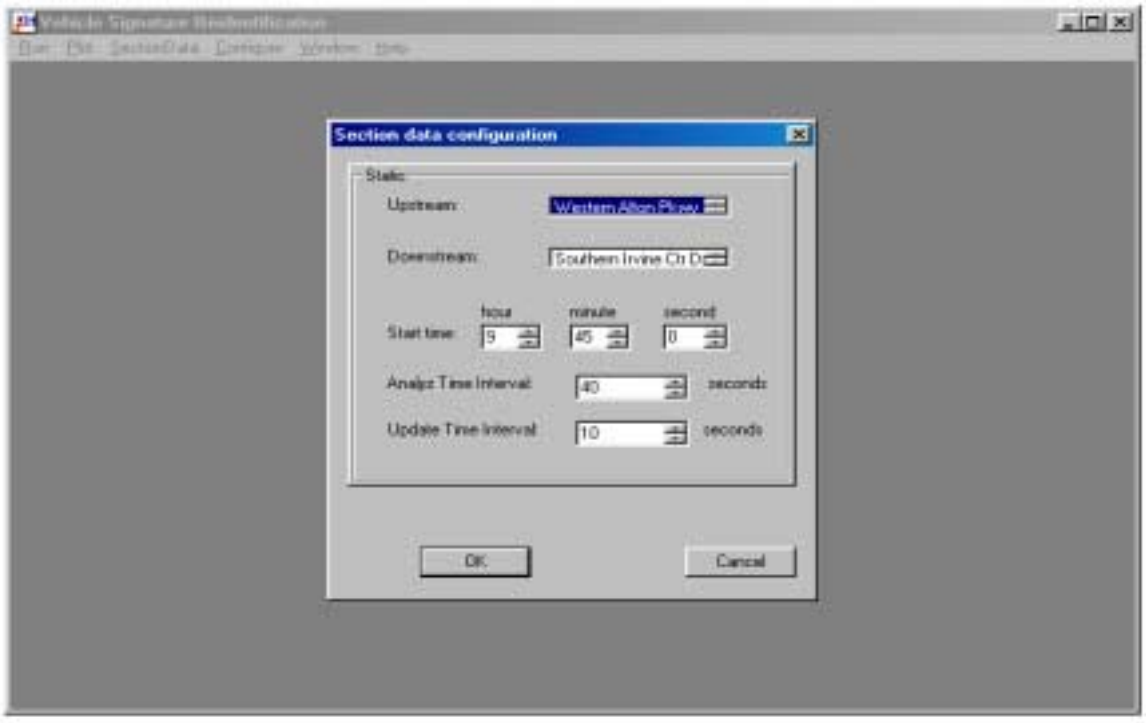

Figure 5.4 Section data configuration

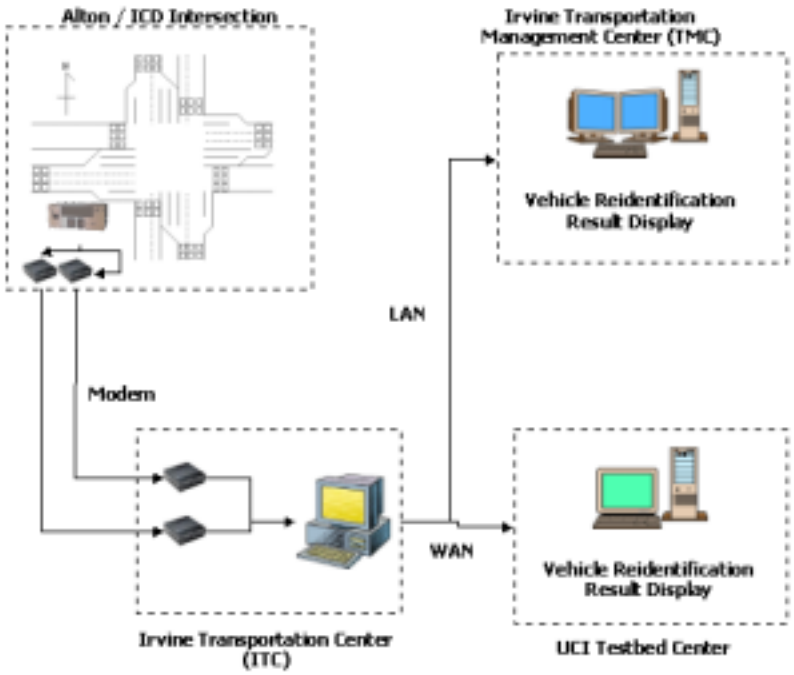

Figure 5.5 Data transmission architecture from Alton/ICD to Irvine TMC

Figure 5.6 On-line vehicle reidentification system workstation at the City of Irvine TMC

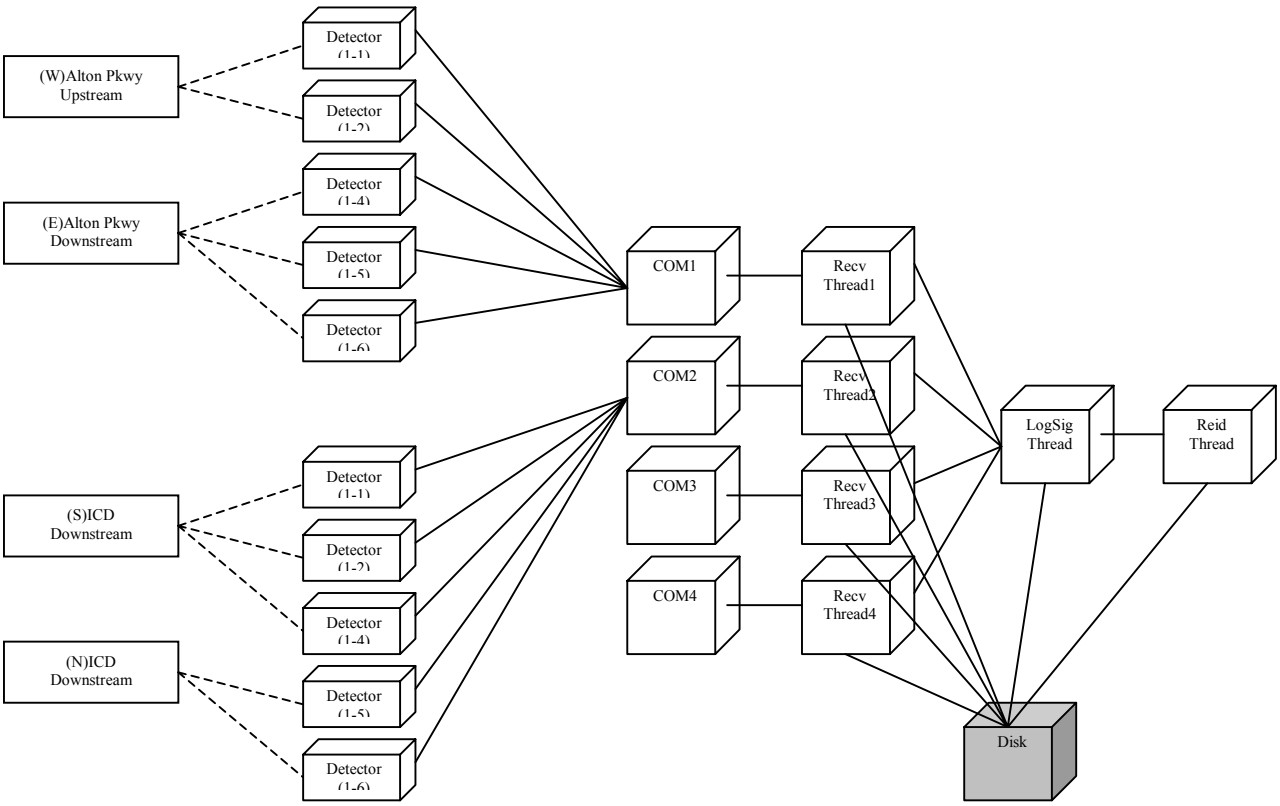

Figure 5.7 Reidentification algorithm architecture

CHAPTER 6 REAL-TIME WEB-SITE DEVELOPMENT AND FIELD COMMUNICATIONS

6.1 INTRODUCTION

As noted in the previous chapter, it was decided to develop an internet-based approach in order to provide real-time vehicle reidentification and traffic performance data to interested remote users. This chapter summarizes the main elements of this effort, including field processing and communications, and the development of a prototype web-site.

6.2 FIELD PROCESSING AND COMMUNICATION

6.2.1 Environmentally Hardened Field Computer

Because of the limitations of the field 2070 controller at the Alton/ICD intersection, it was decided to install an industrial PC in the controller cabinet to perform on-line data acquisition, signature processing, vehicle reidentification and calculation of basic traffic performance characteristics. Due to the potentially high temperatures inside the controller box, an environmentally hardened computer is required in order to perform the real-time data processing and reidentification on-site. Figure 6.1 shows the environmentally hardened PC that was installed in the controller box. This unit follows City of Irvine guidelines for such applications, and houses an 850Mz Pentium III processor, 256MB RAM and a 20GB hard drive, running under Windows 2000.

6.2.2 Ricochet Modem[1]

Because high-speed DSL phone service could not readily be installed at the cabinet, Metricom wireless internet service was selected, using a Richochet modem. In this study, a USB Metricom Ricochet GS modem was use. The modem is a small, external device (roughly 5.0 by 3.5 by 1.0 inch) that weighs about 10 ounces. The modem also contains a removable, rechargeable lithium ion battery and a transportable AC adapter. In general the upload speed (about 110 Kbps) is higher than that for downloading (about 70 Kbps). Several Metricom Ricochet modems are shown in Figure 6.2 .

[1] During Fall 2001, Metricom service ceased. Alternative field communication options are being investigated in collaboration with Caltrans and the City of Irvine.

Figure 6.1 Environmentally hardened computer

Figure 6.2 Metricom ricochet modem

6.3 WEB-SITE DEVELOPMENT

A prototype web-site for internet access to real-time data by operating agencies, UCI researchers, and others is discussed in this section.

6.3.1 Database and Data Flow

As illustrated in Figure 6.3, reidentified section data is aggregated into regular time intervals, in most cases acceptable minimum intervals, at the remote sites. Currently, only one remote site exists for the Alton/ICD intersection, but one freeway site, and possibly others, will be added in the near future. Therefore, the data sender/receiver was coded to account for these possibilities. Aggregated data is sent to the data center at UCI via a wireless internet connection and received by the data collection server located at the data center. The database server parses and stores the sent data. The web server queries data from database, performs more aggregation if needed and presents data in tables and graphs to users. The database is also designed to address future data from different and multiple detectors. For efficient and high speed algorithm operation on-site, the aggregated data is sent continuously, and the processed individual raw vehicle signatures are stored on-site during the day. The stored signature data are transmitted at night when both intersection traffic and the website load are relatively light.

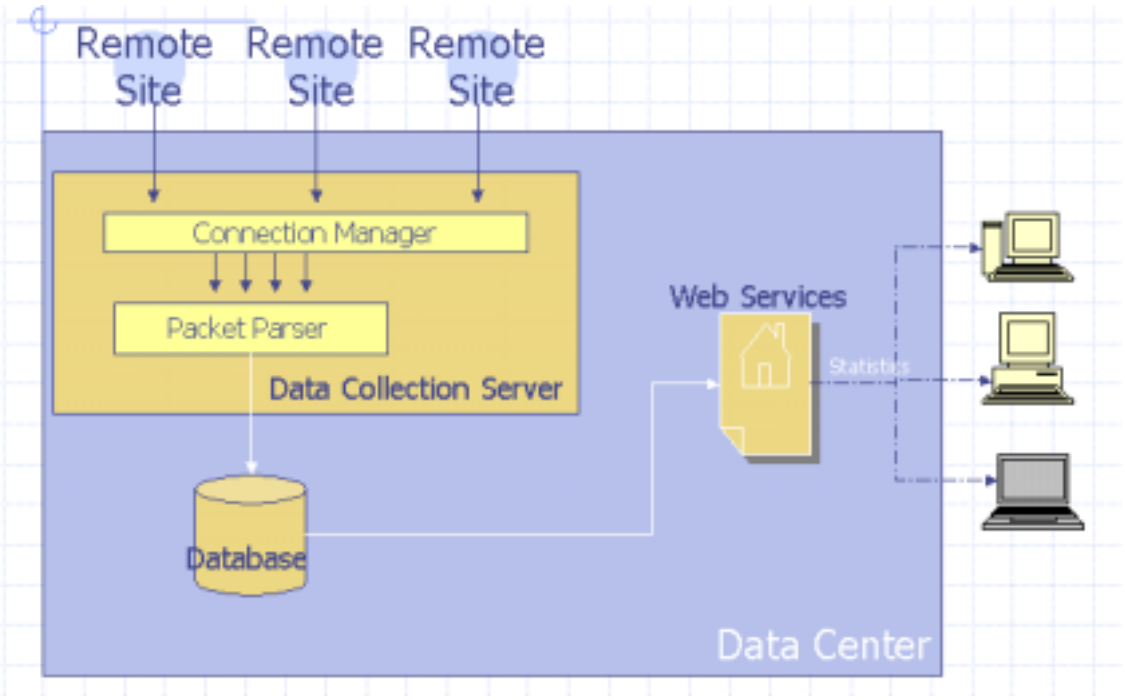

Figure 6.3 Data flow architecture

Currently, the data collection, database, and web servers are integrated into a single server that is Intel-based (dual Pentium 1000MZ) running Windows 2000. These web services could be distributed over multiple servers in the future. In terms of software, the data collection server uses Java, the database server uses Microsoft SQL server,and the web server uses ColdFusion.

6.3.2 Web-Site (http://www.its.uci.edu/reid)

Figure 6.4 represents the introductory screen for the web-site and explains to the user the data that are available on the website. Section data (such as travel time), refer to data that are obtained directly or derived from the reidentified data between upstream and downstream locations, while point data refer to data such as volume and local speed at one location. At each upstream station, point data are displayed. For the section data case, the data are displayed downstream for each movement (through, right and left).

Based on the user's query, sometimes the data need to be aggregated when the analysis interval is longer than the minimum interval used for sending data from the field. For example, aggregated intersection data are currently sent from the field every 60 seconds. If the user requests an analysis interval of five minutes, then five time steps of one minute interval data need to be aggregated, as indicated below.

$$SD^k = \frac{\sum_{i=0}^{n} (RVC_i^m \bullet SD_i^m)}{\sum_{i=0}^{n} RVC_i^m}$$

$n = \frac{k}{m}$, an integer

where

SD^k : Section data of "k" interval

SD_i^m : Section data of "m" interval

RVC_i^m : Reidentified vehicle pair count at "m" interval

k : Query interval

i : Minimum Interval

Figures 6.5 and 6.6 present some example pages from the current prototype web-site, including display of sample real-time 2-minute data for Alton Parkway eastbound, and plots for the same data, respectively.

Figure 6.4 Introductory web-site page for Alton Parkway and Irvine Center Drive intersection

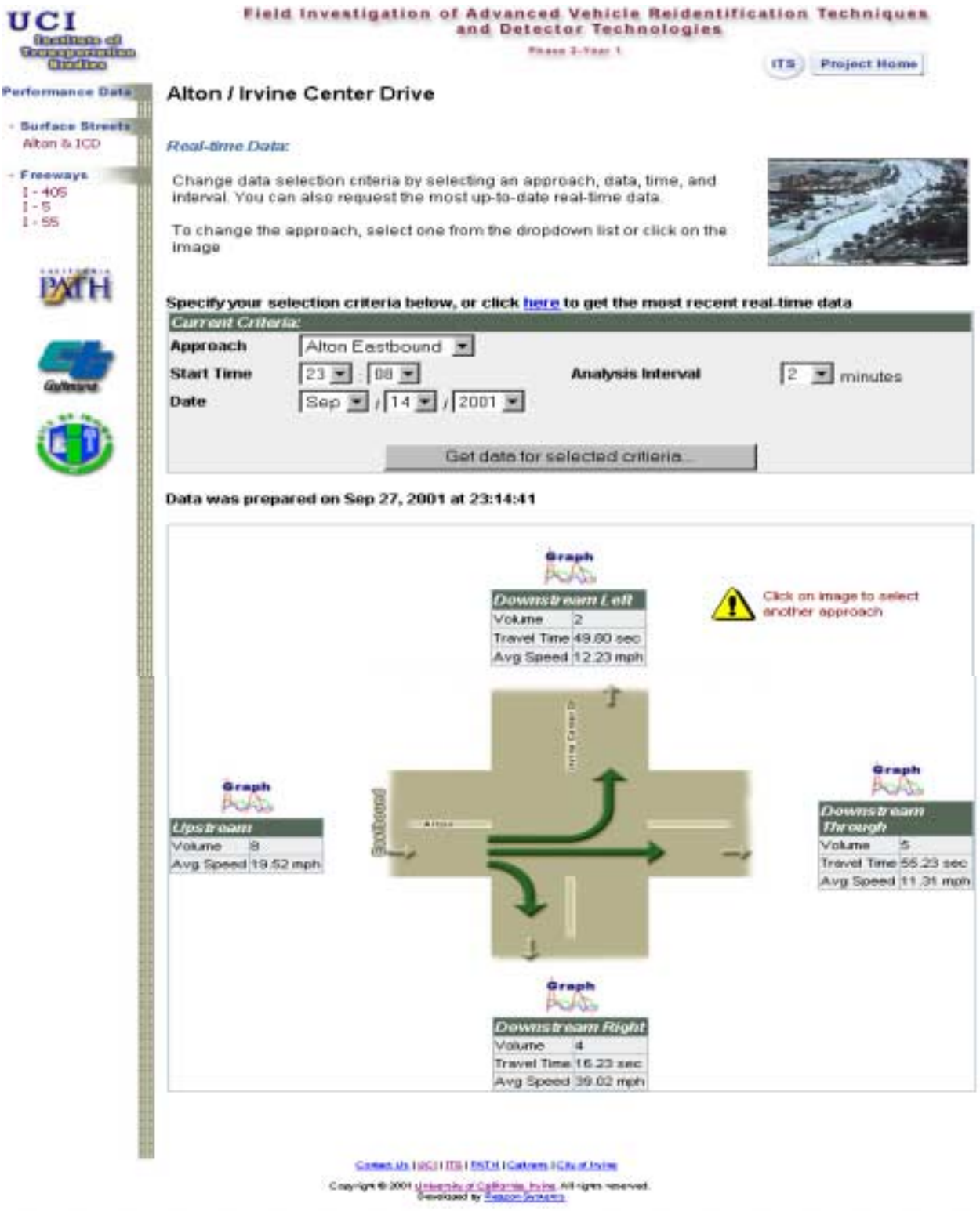

Figure 6.5 Web-site display of example real-time 2-minute data for Alton Parkway eastbound

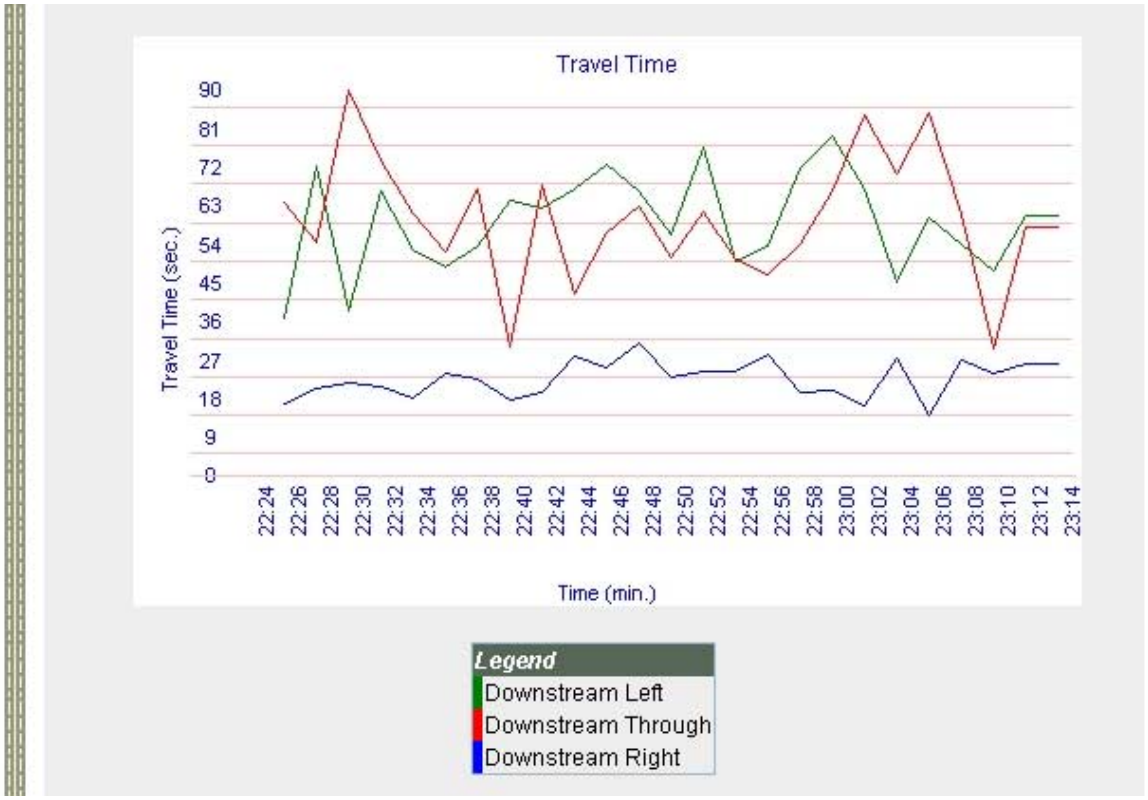

Figure 6.6 Example web-site plots for the criteria in Figure 6.5

CHAPTER 7 COMPARATIVE ANALYSIS OF PROTOTYPE IST-222 DETECTOR CARD

7.1 INTRODUCTION

This chapter describes a comparative analysis of control vehicle signatures using two different high-speed scanning detector cards: a prototype version of the IST-222 card from Inductive Signature Technologies, Inc., and the 3M card that has been used by the authors in vehicle reidentification studies in both MOUs 224 and 336. The purpose of these comparisons was to investigate the signature repeatability of the IST-222 card, and its feasibility for future vehicle reidentification use.

Because the sample rate of the IST-222 card can be variably set to generate up to several orders of magnitude more sample data in a vehicle signature than currently available high-speed scanning detector cards, such as the 3M card, it is hoped that improved vehicle reidentification results will be achievable due to the more detailed signatures. The IST-222 card also has a USB output port which greatly facilitates data collection.

7.2 DATA COLLECTION

In order to test vehicle signature repeatability and feasibility, the two different detector cards were investigated using control vehicles consisting of several different vehicle types. The cards were connected to the controller located at Alton/ICD intersection in the City of Irvine. Figure 7.1 describes the double loop and card installation layout. Five different control vehicle types were used for data collection: passenger car, van, mini van, pickup truck, and cargo van. The data were collected during a morning non–peak period on May 28th, 2001. The data collection period was divided into two periods, with period one from 9:00-10:00am and period two from 10:15-10:55am. However, due to an IST software problem, the IST-222 data from 9:26 AM to 10:45 AM were lost. Therefore, the total vehicle passes for each vehicle ranged between 30–34 in the case of the 3M detector card and 10–13 for the IST–222 detector card. Figures 7.2-7.6 show the five vehicle types and their corresponding vehicle signatures from each detector card. The figures show that a major difference between the cards is their data sampling rate and consequently, their sampling number of data points in each signature. For the 3M card, a 7 ms (millisecond) sampling rate was used while for the IST-222 card a sampling rate of about 0.25ms was used. Therefore, the sample data from the IST–222 card was approximately 30 times greater than that from the 3M card

It is interesting to note that in the case of the IST–222 card, the front loop signature magnitude tended to be smaller than that from the back loop. The IST-222 card was set to sample at a rate of approximately 4kHz, and operated at a frequency separation of approximately 5kHz. Because the frequency response of the detector circuit is a function of the operating frequency of the detector, the magnitudes of the inductive signatures generated by the two detectors were different. IST has indicated that this can be compensated for by calculating a normalizing coefficient for each detector, and multiplying each element of the inductive signature by the normalizing coefficient prior to output from

the detector. This normalizing coefficient may be determined empirically by simply comparing two signatures produced by the same vehicle and choosing coefficients that will make the signatures match the best, or by using an equation which accounts for the electrical parameters and operating conditions of the loop detector.

7.3 VEHICLE SIGNATURE COMPARISON

7.3.1 Selected Features

In this study, four specific vehicle signature features were selected to evaluate each detector card's repeatability and feasibility, as illustrated in Figure 7.7. These features were the maximum signature magnitude, (electronic) vehicle length, shape parameter, and difference in the area of the normalized front and rear loop signatures. Figure 7.8 presents the shape parameter and vehicle length ranges (in m.) obtained in our previous studies. The shape parameter, which is related to the signature skewness, shows an obviously different range in the case of a vehicle and trailer combination. This can be easily seen from Figure 7.9.

The coefficient of variation was calculated as an index of the variability of each feature. The coefficient of variation is useful when comparing the variability of two or more data sets that differ considerably in the magnitude of the observations, and is defined by the following equation:

$$CV = \frac{STD}{M} 100\ \%$$

where

CV : Coefficient of Variation, %

STD : Standard Deviation

M : Mean

7.3.2 Comparative Results

The comparative results for the four features, five vehicle types, and 3M and IST-222 detector cards are presented in Figures 7.10-7.12. As already noted, a clear distinction between the two cards exists due to a significant difference between the front and back loop maximum magnitudes for the IST-222 signatures. From examination of the coefficients of variation, the IST-222 signatures were often more "reliable" compared with the 3M signatures. Also, the normalized IST-222 front and back loop signatures were more alike than those for 3M, except for the van control vehicle. Vehicle length was best measured with the front loop IST-222 signatures, and these length measurements were highly repeatable, as evidenced by the low coefficients of variation.

7.4 CONCLUDING COMMENTS

The prototype IST-222 card shows considerable promise for use in future vehicle reidentification studies. However, the differences found between the front and back loop maximum magnitude renders the current prototype IST-222 detector card unusable for our intersection vehicle reidentification algorithms (although IST has indicated that this problem can be addressed readily). The fact that the normalized front and back loop IST-222 signatures were more similar than the 3M signatures could lead to an improvement in vehicle reidentification algorithm performance, however, if this also holds for different detector stations such as upstream and downstream stations (and the magnitude problem above is fixed). Further analysis of updated and enhanced IST-222 cards will be undertaken in the future, as the cards become available from IST, Inc.

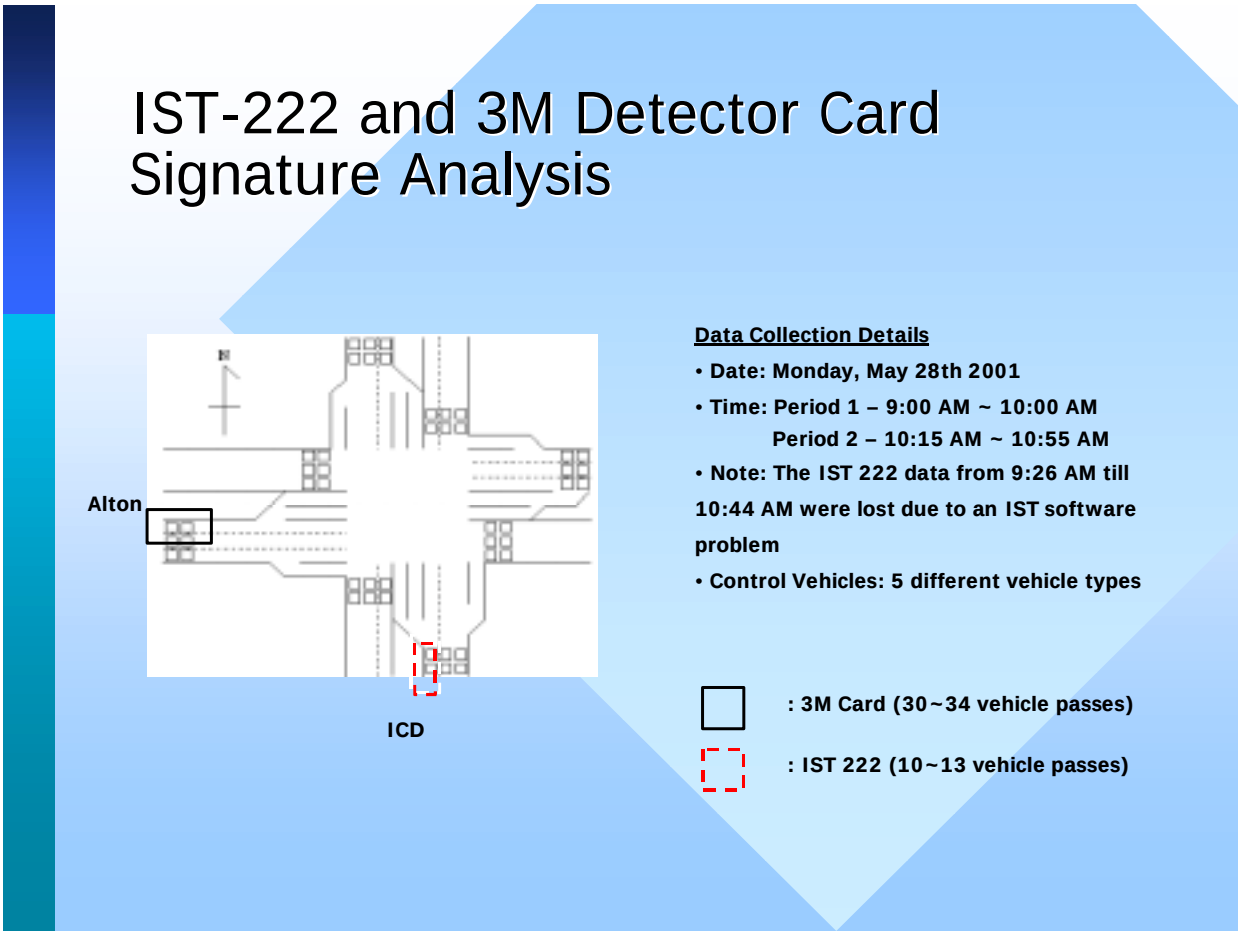

Figure 7.1 Data collection details for 3M and IST-222 detector card field study

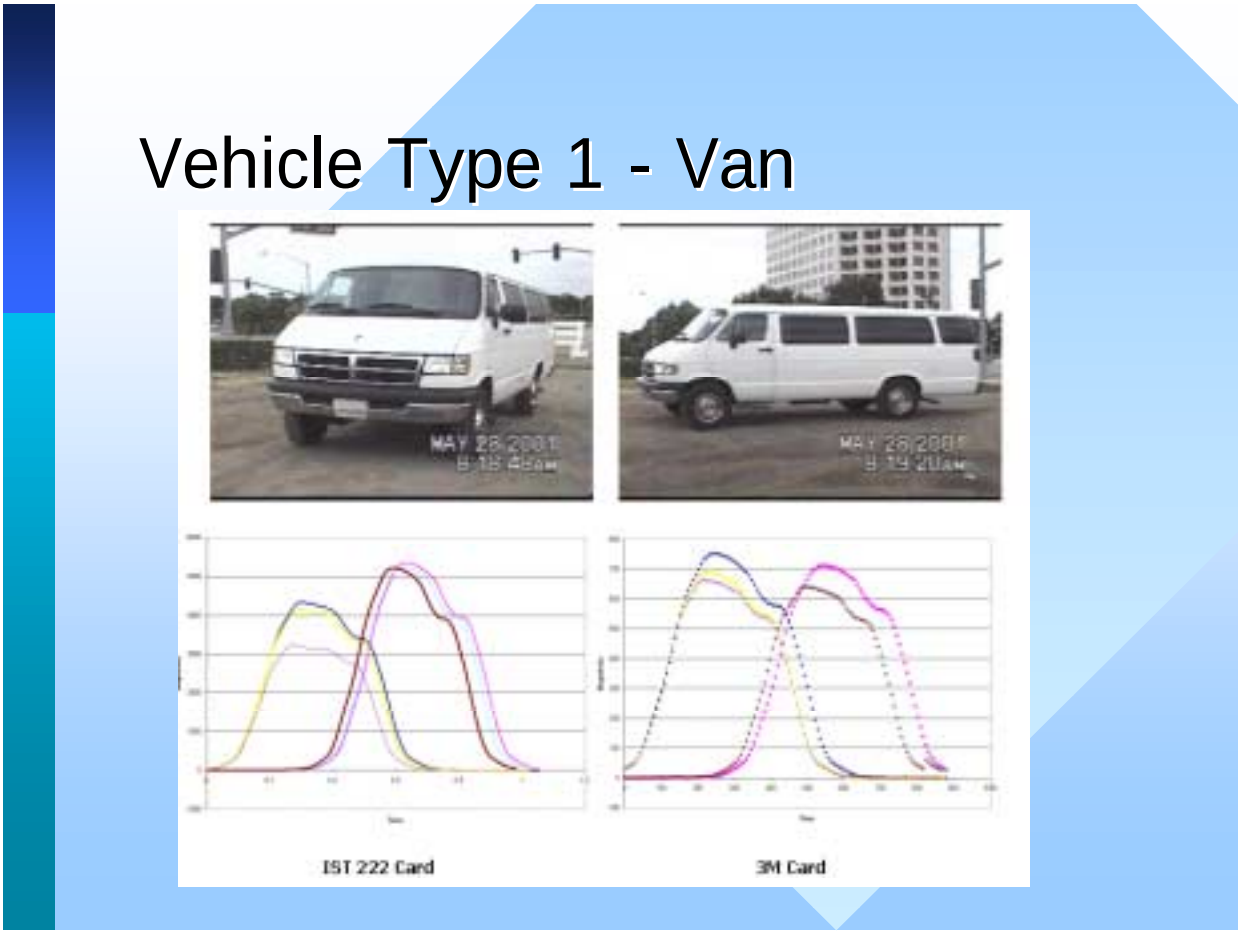

Figure 7.2 Vehicle type 1 and its corresponding signatures

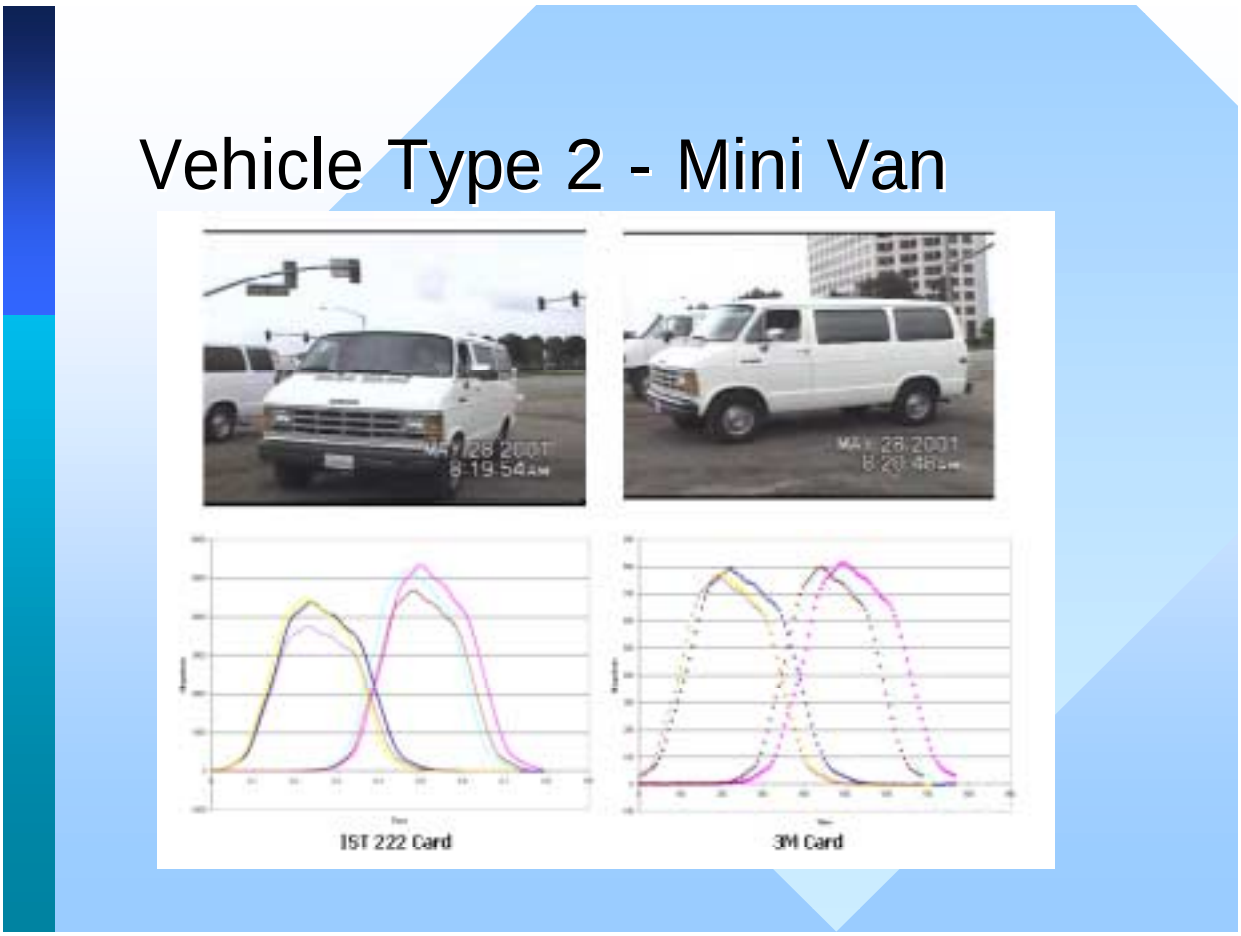

Figure 7.3 Vehicle type 2 and its corresponding signatures

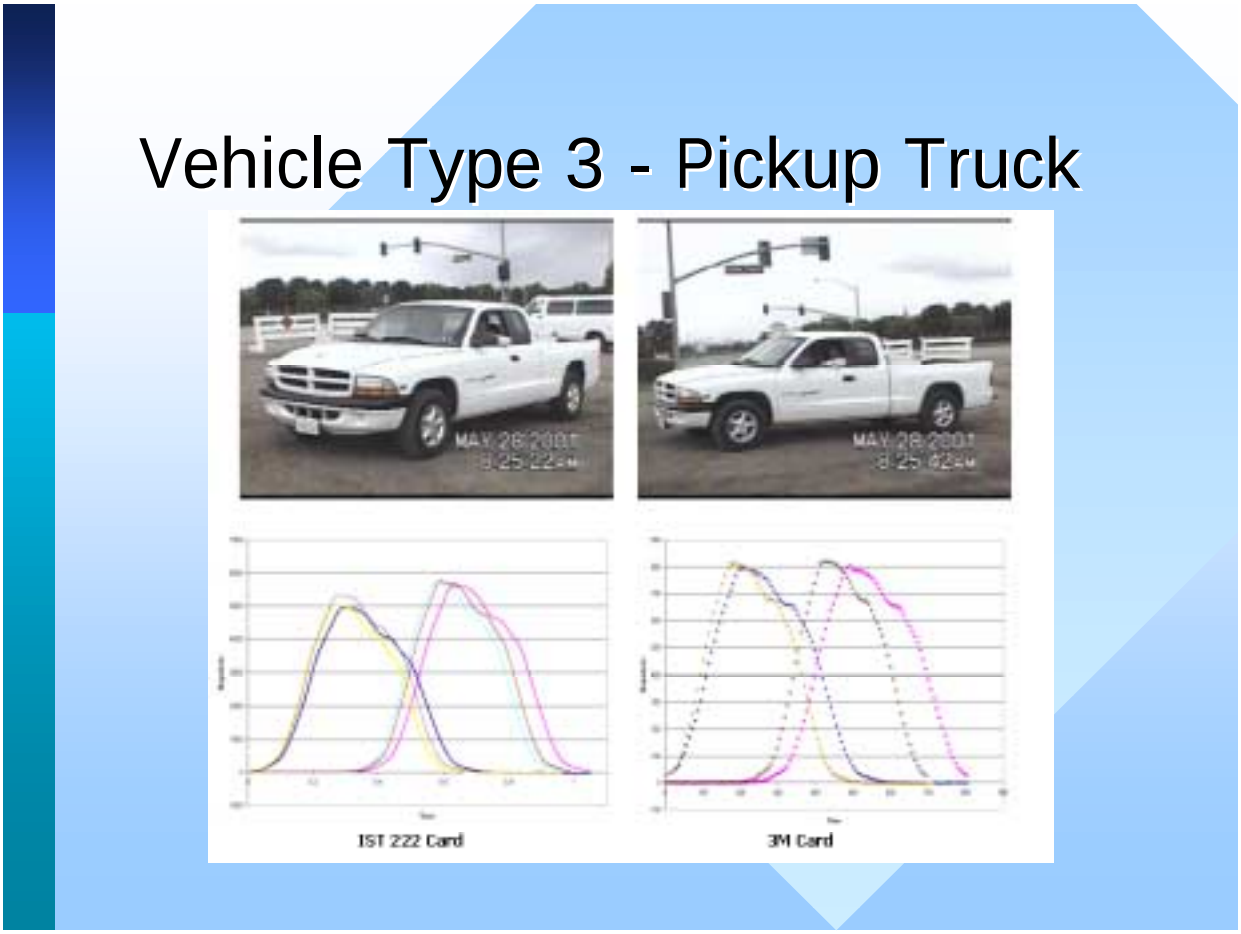

Figure 7.4 Vehicle type 3 and its corresponding signatures

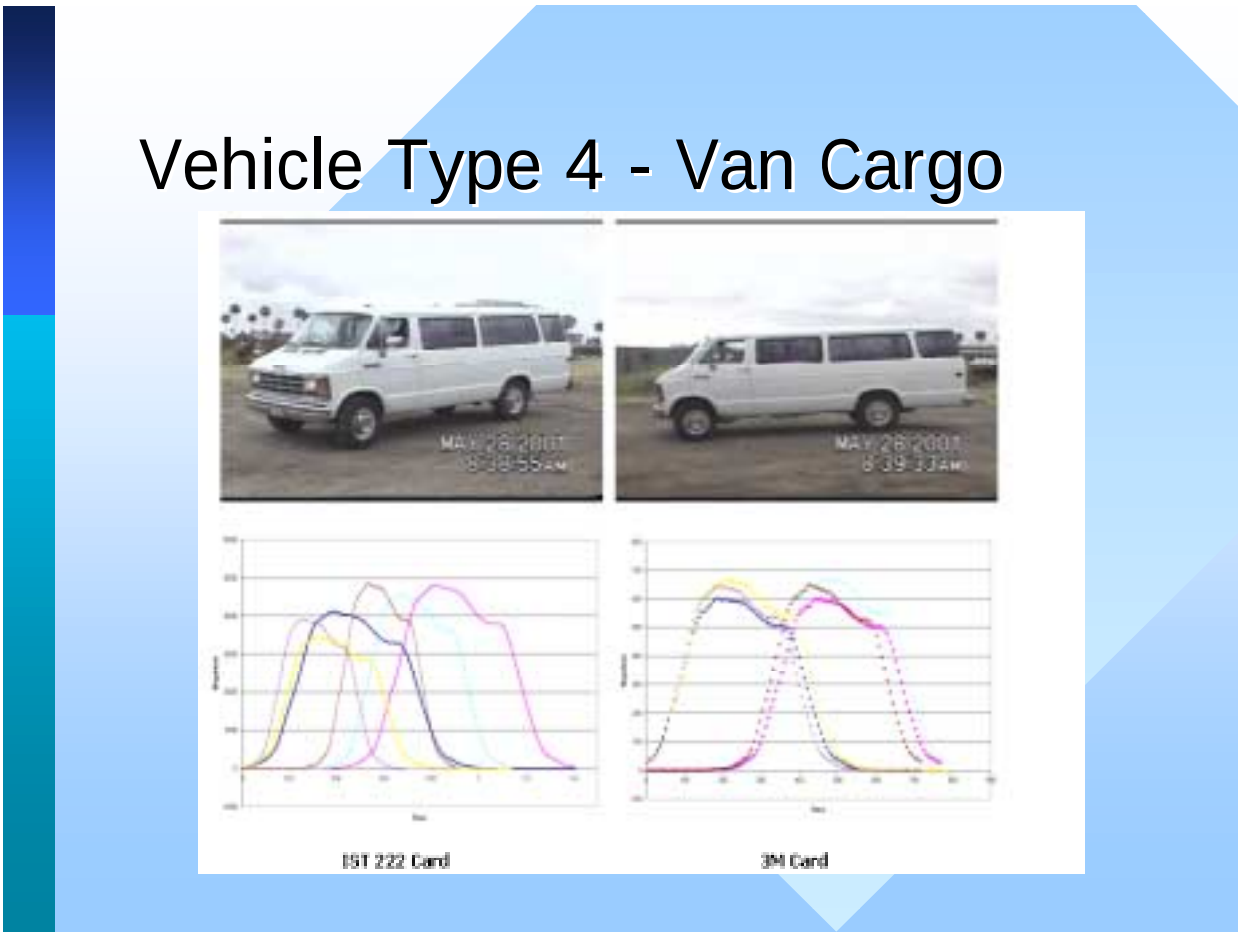

Figure 7.5 Vehicle type 4 and its corresponding signatures

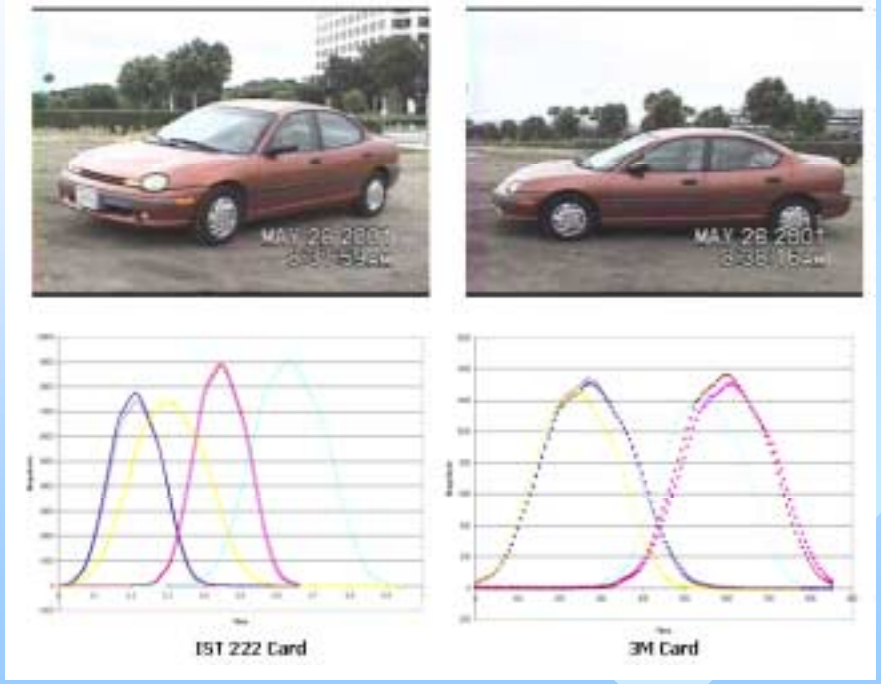

Figure 7.6 Vehicle type 5 and its corresponding signatures

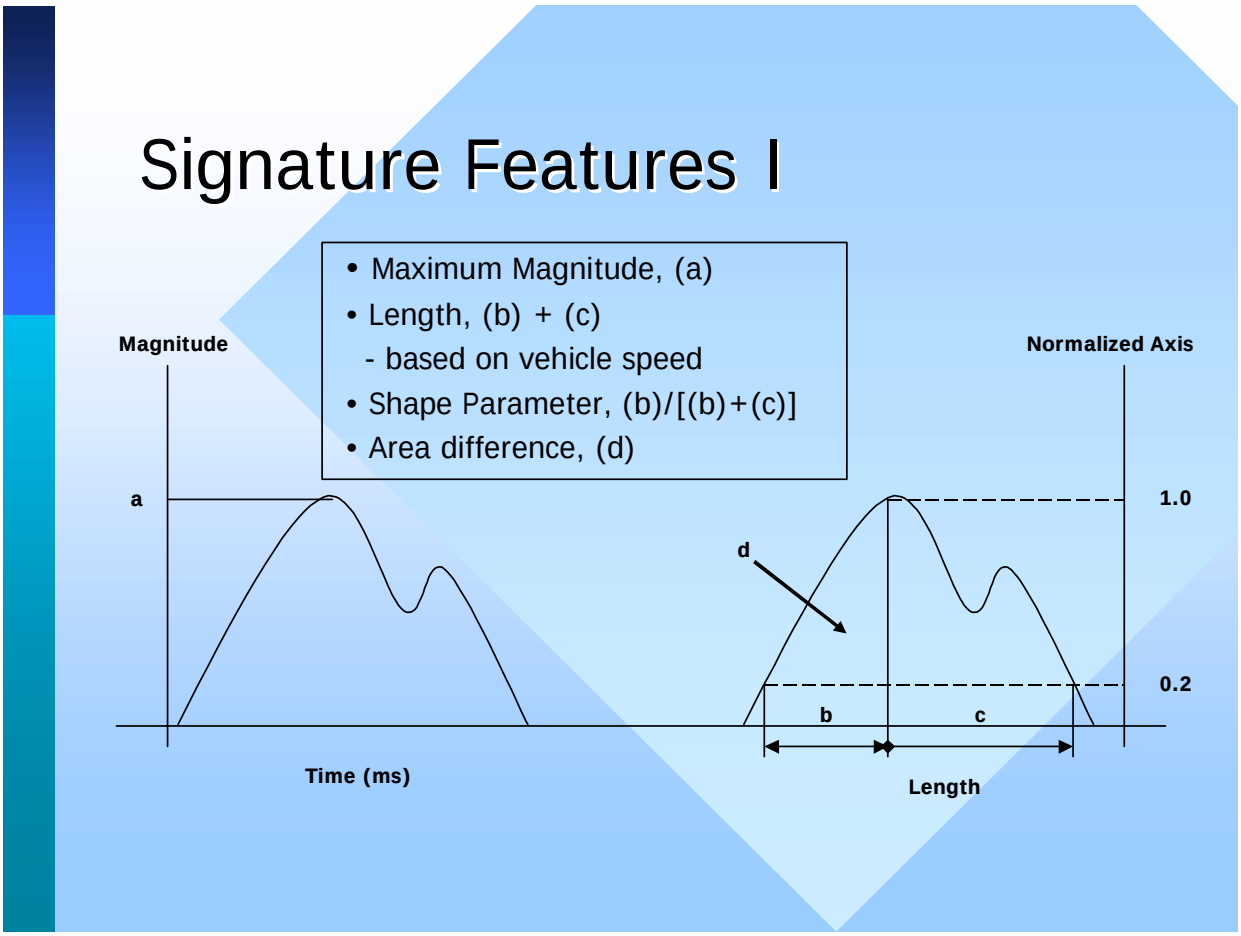

Figure 7.7 Four signature features used in the study

Signature Features II

- Typical shape parameter and length (m) ranges

Features	Shape Parameter	Length
Passenger Car	0.49 ~ 0.51	3.7 ~ 5.4
Sport Utility Car	0.32 ~ 0.53	3.8 ~ 6.0
Van	0.36 ~ 0.47	5.1 ~ 6.4
Trailer	0.1 ~ 0.28	Over 8

Figure 7.8 Shape parameter values from previous studies

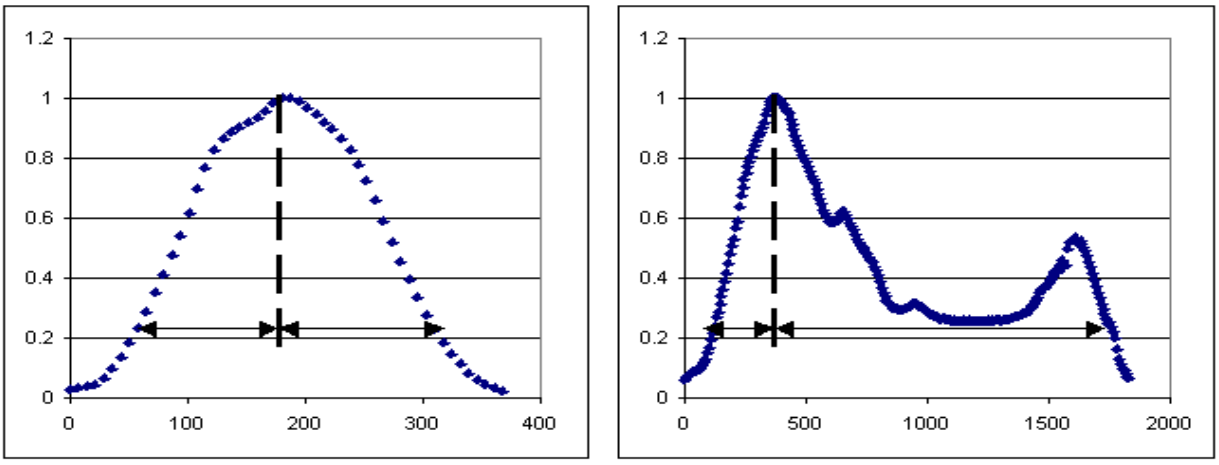

(a) Passenger car example signature

(b) Vehicle with trailer example signature

Figure 7.9 Example signatures for passenger car and vehicle with trailer

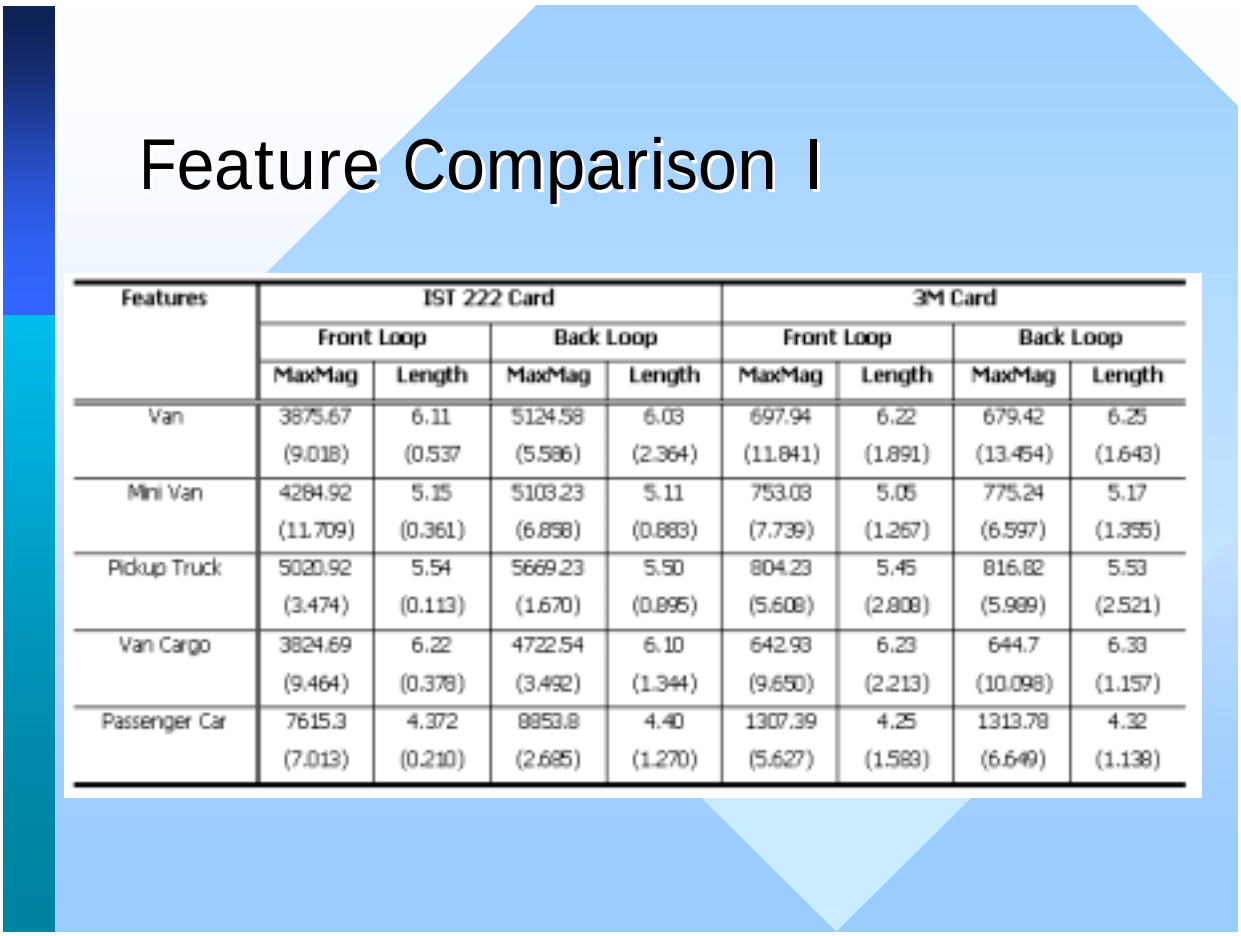

Features	IST 222 Card				3M Card			
	Front Loop		Back Loop		Front Loop		Back Loop	
	MaxMag	Length	MaxMag	Length	MaxMag	Length	MaxMag	Length
Van	3875.67 (9.018)	6.11 (0.537	5124.58 (5.586)	6.03 (2.364)	697.94 (11.841)	6.22 (1.891)	679.42 (13.454)	6.25 (1.643)
Mini Van	4284.92 (11.709)	5.15 (0.361)	5103.23 (6.858)	5.11 (0.883)	753.03 (7.739)	5.05 (1.267)	775.24 (6.597)	5.17 (1.355)
Pickup Truck	5020.92 (3.474)	5.54 (0.113)	5669.23 (1.670)	5.50 (0.895)	804.23 (5.608)	5.45 (2.808)	816.82 (5.999)	5.53 (2.521)
Van Cargo	3824.69 (9.464)	6.22 (0.378)	4722.54 (3.492)	6.10 (1.344)	642.93 (9.650)	6.23 (2.213)	644.7 (10.098)	6.33 (1.157)
Passenger Car	7615.3 (7.013)	4.372 (0.210)	8853.8 (2.685)	4.40 (1.270)	1307.39 (5.627)	4.25 (1.583)	1313.78 (6.649)	4.32 (1.138)

Figure 7.10 Detector card feature comparison, showing means and coefficients of variation for signature maximum magnitude and vehicle length (m)

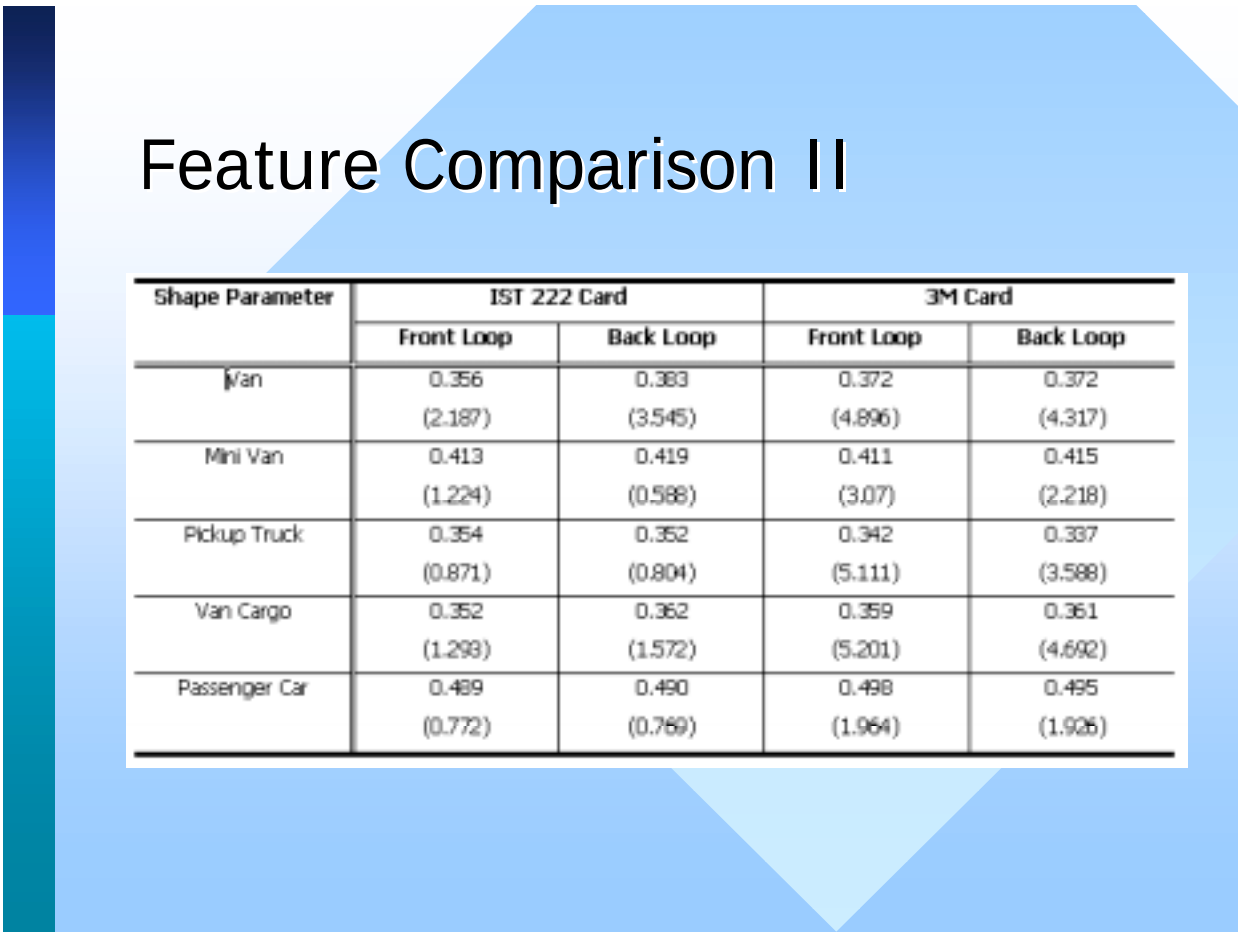

Shape Parameter	IST 222 Card		3M Card	
	Front Loop	Back Loop	Front Loop	Back Loop
Van	0.356	0.383	0.372	0.372
	(2.187)	(3.545)	(4.896)	(4.317)
Mini Van	0.413	0.419	0.411	0.415
	(1.224)	(0.588)	(3.07)	(2.218)
Pickup Truck	0.354	0.352	0.342	0.337
	(0.871)	(0.804)	(5.111)	(3.588)
Van Cargo	0.352	0.362	0.359	0.361
	(1.293)	(1.572)	(5.201)	(4.692)
Passenger Car	0.489	0.490	0.498	0.495
	(0.772)	(0.769)	(1.964)	(1.926)

Figure 7.11 Detector card feature comparison, showing means and coefficients of variation for shape parameter

Feature Comparison III

Area Difference	IST 222 Card	3M Card
Van	18.749 (33.242)	5.777 (69.686)
Mini Van	4.974 (42.891)	8.953 (19.701)
Pickup Truck	3.152 (45.781)	9.435 (27.848)
Van Cargo	10.853 (25.356)	13.643 (34.147)
Passenger Car	3.392 (56.254)	6.112 (37.753)

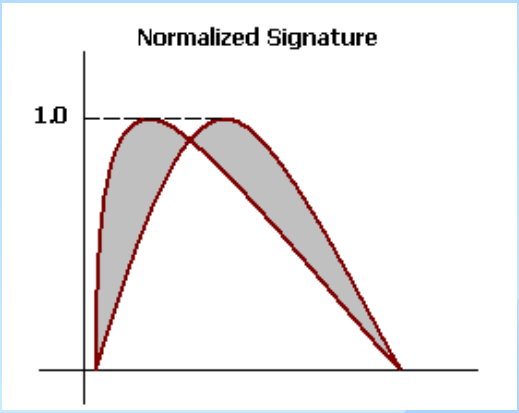

Figure 7.12 Detector card feature comparison, showing means and coefficients of variation for differences in normalized signature areas

CHAPTER 8 VIDEO IMAGE PROCESSING FOR DETECTOR DATA FUSION

8.1 INTRODUCTION

This chapter presents the results of an initial study (to be continued in Phase II of the research) of video image processing for future detector data fusion of video and loop signature data. Such data fusion is expected to lead to improved vehicle reidentification and improved accuracy of the resulting real-time traffic performance data.

8.2 VIDEO AND SIGNATURE DATA

At the time of signature data acquisition in this and previous research by the authors, video footage of the traffic was also recorded for ground truth purposes. In PATH MOU 224, four video cameras recorded two lanes of traffic in each of the upstream and downstream locations. From this continuous video footage, one can visually identify many of the vehicles by type and color. The goal of this element of the research was to develop software than could automatically identify characteristics of vehicles that were passing over the loop detectors at certain times. The first step in this process is to capture the video data into the computer. To do this, we used Live! hardware from Nogatech. This hardware was connected the S-video port of a VCR and to the USB port of a computer. MGI VideoWave SE+ software was used to access the video signals coming from our Live! Hardware. Initially, the default software options were used to capture the still images of traffic. Originally, the video was only recorded for the purpose of identifying the vehicles visually. Therefore issues such as lighting, angles, and centering the frame of vision were not considered a priority.

8.3 VIDEO IMAGE PROCESSING

8.3.1 Background Subtraction Process

The theory behind the background subtraction process was straightforward. Two images were captured on the same section of road. One image had no vehicles present, and was designated as the background image. The other image did have vehicles present. The software read each of these image files and stored the data as a variable of bitmap class. After investigation, it was verified that the software created all bitmaps of the same pixel height and width. Therefore, the same coordinates in each image should represent the same physical location. A comparison is then performed between the two variables. Specifically, each pixel of the same coordinates in each of the image is compared by its RGB values. First, a pixel in the image is examined to see if it has the same RGB values as the pixel in the identical location in the background image. If so, that pixel in the image was then changed, to have an RGB value of 000, all null. In theory, all of the pixels representing the background should be identical in each of the two images. Therefore, we would expect that the resulting image would have a vehicle surrounded by null pixels. In actuality, we found that only about 30-40% of the image would be blacked out.

Comparison Thresholds

It was found that blacking out pixels in the image when they identically matched the background did not produce satisfactory results. Here, the difference between each of the Red, Green, and Blue (RGB) values was zero. The images contained 256^3 different colors. It seemed to be reasonable that with 16.8 million possible colors, there could easily be some variation in the colors present in two images of the same background. Thus, the difference threshold between the two RGB values was increased from zero on up. Recording the percentage of pixels in the image that were blacked out, we developed curves from which we could pick the best possible comparison threshold values. Figure 8.1 shows several examples of curves developed from analyzing the background subtraction process on various images. Under values of 30, a great deal of the image that is not the vehicle is present. Around values of about 60, the shape of the image is present best, as most of the background has been removed. Finally, values around 100 and higher are best to find colors present in the vehicle. Figure 8.1 shows the results of comparing the percentage of blacked out pixels with the comparison thresholds for various vehicles.

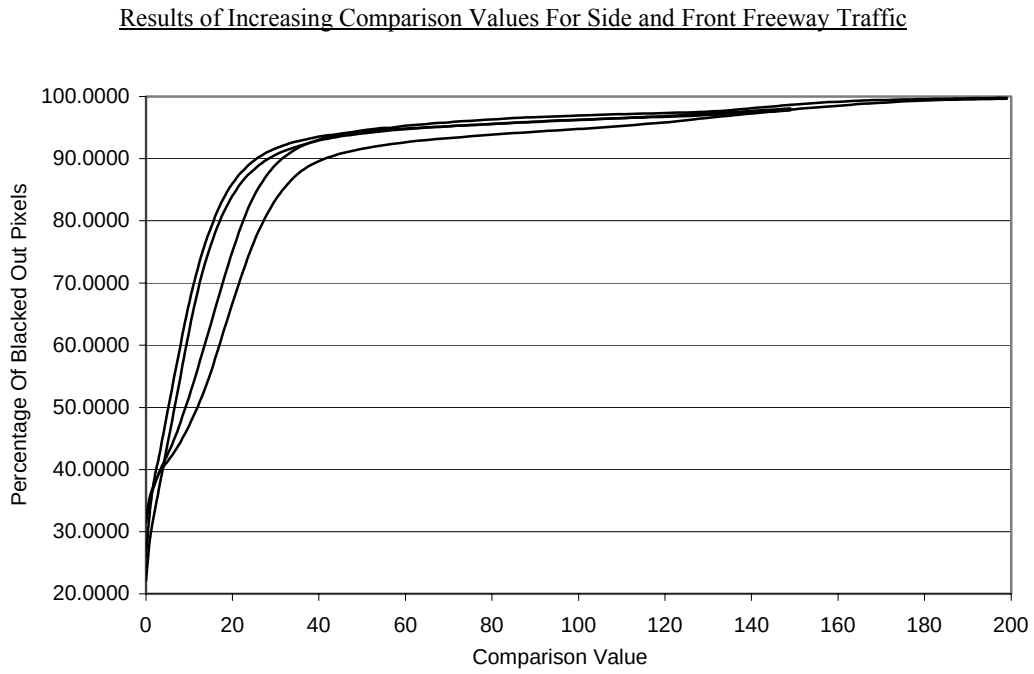

Figure 8.1 Adjustment of comparison threshold

Investigation of Acquisition Properties

The next step was to determine if we could improve on the background subtraction process. Much of the image that was not blacked out seemed to have glare. Therefore we took a step back to examine the process of capturing the

images. We decided to vary the brightness and contrast options when capturing images, effectively adjusting the dynamic range of the images. Originally, we used the commercial software's default settings when capturing images. At this point though, it was decided some investigation of those properties was warranted. New images were captured with the image settings for contrast and brightness and were both varied higher and lower from the middle setting in every combination. Background subtraction was then run to get comparison threshold curves for each set of values for brightness and contrast of an image. Excessive values of brightness and contrast together proved to produce less attractive curves. The middle ranges of each setting produced the sharpest curve that would be best for image processing. Originally, the software's default setting for capturing images from the video had both the brightness and contrast between middle and high values. Ideally, in the future when recording the video, lighting will be taken into consideration so that the images can be processed more easily. Figure 8.2 shows the effects of brightness level on background subtraction.

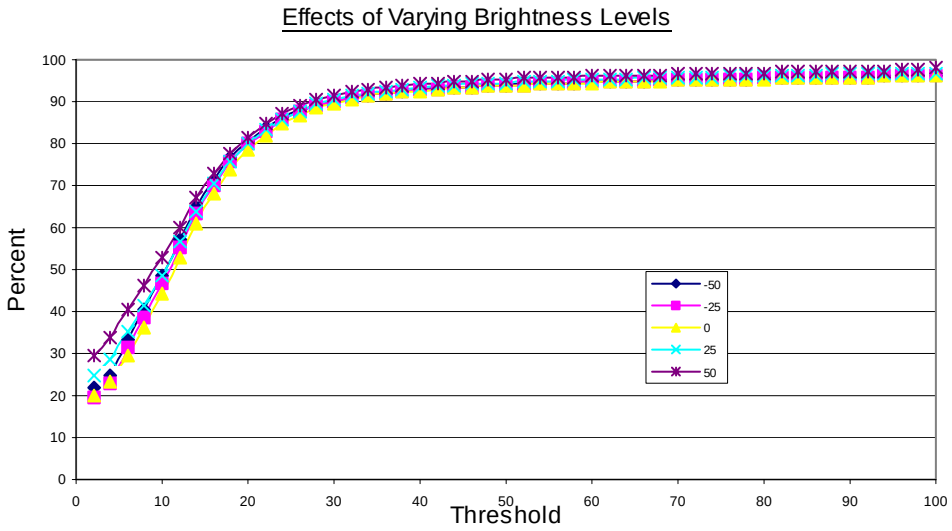

Figure 8.2 Effects of brightness

8.3.2 Color Extraction

The first thing we wished to extract from the images was color of the vehicle present in the image. If this information could be determined, it could theoretically increase the accuracy of the rest of the reidentification process. We kept track of every color that was present in an image after the background subtraction took place. This yielded thousands of colors for any image. Nearly every color present only occurred a handful of times. Again, we realized we would have a problem similar to the one we encountered during the background subtraction. Namely, with 16.8 millions possible colors, it would be unlikely that two images of the same vehicle in different locations would have exactly the same color. When colors were extracted in this fashion, the colors present most were all some value of a shade of the vehicle in question. For example, Table 8.1 is the top of a chart of the colors present in an image. In this case, there were 4600 colors present in the 5400 pixels that were not blacked out.

Table 8.1 Sample vehicle color information

RGB Number	Count	Color
255 255 255	23	Black
254 254 254	14	Black
253 253 253	8	Black
167 164 255	7	Blue
115 112 219	7	Blue
113 111 218	6	Blue
253 253 255	6	Black
159 169 255	5	Blue
166 177 255	5	Blue
147 126 255	5	Blue
106 098 219	5	Blue

8.3.3 Color Quantization

After our first trials with color extraction, we discovered that color extraction had potential. Next, we determined what information and what quality we needed from the extraction process. Instead of using every color in the RGB three dimensional cube, we decided to use some quantization of the colors. Instead of 16.8 millions colors, we quantized that information into 8 colors as a first trial. A count was kept of how many pixels fit into each of the quantized values. From the count, a percentage of that color out of the total pixels left after background subtraction was calculated. Figure 8.3 illustrates this process graphically.

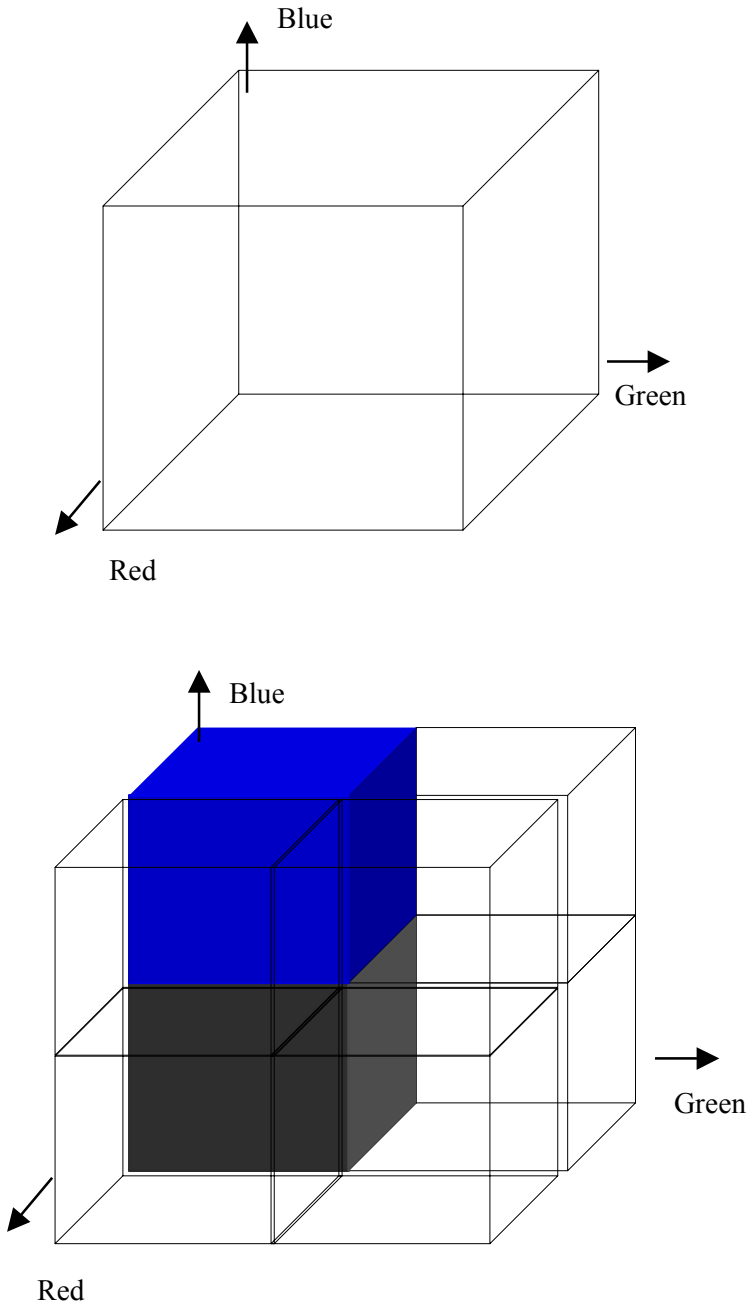

Figure 8.3 Graphical illustration of the quantization process

Next, we captured samples of 20 vehicles upstream and downstream. Running a color extraction on each of the images, we took the 5 colors present "most", or the colors with the highest percent values. An example of this is shown in Table 8.2 with the percentage values removed. Out of these 20 pairs of images, 65% of the colors present in one of the pairs of images were present in the other at the same rank. Also, out of the top 5 colors present in the images, the pairs shared 85% of the colors.

Table 8.2 Sample color levels for a pair of vehicles

ID	Site	Ln	Max Color	2nd Color	3rd Color	4th Color	5th Color
20	Up	1	64 64 64	192 64 64	192 192 192	64 64 192	192 64 192
20	Down	1	64 64 64	192 192 192	192 64 64	64 64 192	192 64 192
Same Rank			Yes	No	No	Yes	Yes
Value Present			Yes	Yes	Yes	Yes	Yes

Of greater interest though were the similarities of the actual percentage values. At this point, it was theorized that the percentage values of the colors would match up best to the same vehicle. The code was rewritten to test out this theory. A function that would calculate the percentage values of the colors in each of two images was needed. A sum difference squared operation was performed on the percentage values of the colors found in each of the two images. This gave a numerical comparison of the colors present in each of two images, as shown in Table 8.3.

Table 8.3 Sample color levels for a second pair of vehicles

ID	Site	43 43 43 Percent	215 43 129 Percentage	215 43 43 Percentage	129 43 43 Percentage	215 215 215 Percentage
27	Up	38.7536	14.5954	13.9268	7.33417	7.27339
27	Down	40.9724	13.5631	11.3563	11.5018	10.6089

8.4 EXAMPLE IMAGES

Example images are included in the following figures. Figure 8.4 illustrates the process of background subtraction using a side view image from the SR-24 freeway. Figure 8.5 illustrates the process of background subtraction using a rear view image from Alton Parkway. Figure 8.6 illustrates the original image as well as the subtracted image for both downstream and upstream.

8.5 FUTURE APPLICATIONS

The results of this study suggest that the integration of this method of image comparison with the existing reidentification system could possibly be beneficial in increasing the accuracy of reindentification. Further studies of data fusion of different detector outputs will be conducted in Phase II of the research for the purpose of improving vehicle reidentification.

Figure 8.4 Background subtraction process, image one

No Subtraction

Threshold = 20

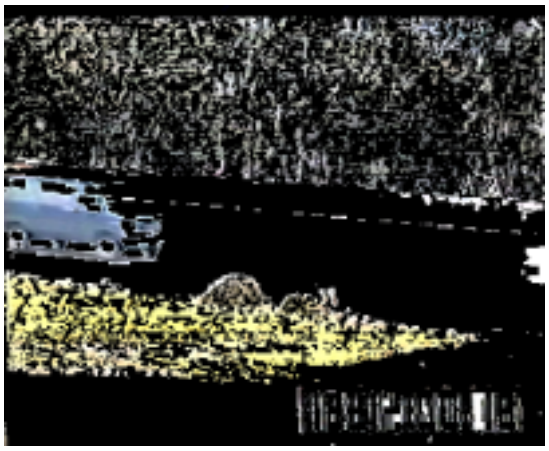

Threshold = 40

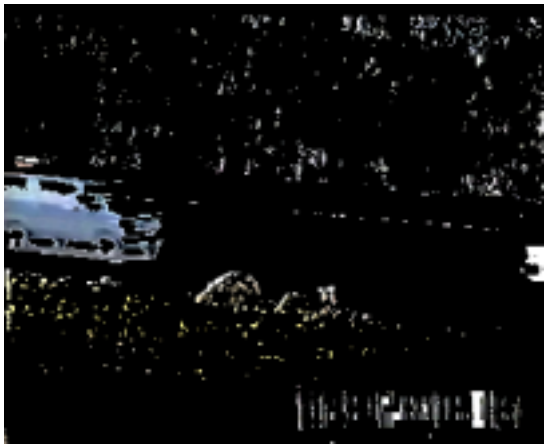

Threshold = 60

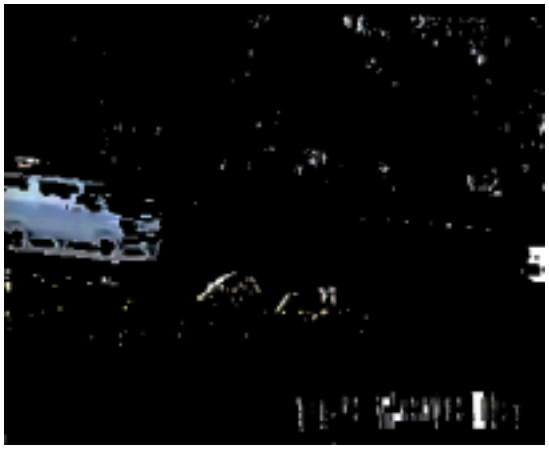

Threshold =80

Threshold = 100

Figure 8.5 Background subtraction process, image two

No Subtraction

Threshold = 20

Threshold = 40

Threshold = 60

Threshold = 80

Threshold = 100

Figure 8.6 Background subtracted images

Vehicle 20 UpStream

Vehicle 20 DownStream

Vehicle 20 UpStream
Post Background Subtraction

Vehicle 20 DownStream
Post Background Subtraction

CHAPTER 9 CONCLUSIONS AND FUTURE RESEARCH

9.1 CONCLUSIONS

This report presents the results of Phase I of a multi-year research effort on "Field Investigation of Advanced Vehicle Reidentification Techniques and Detector Technologies," and extends previous PATH research by the authors on MOU 336 "Section-Related Measures of Traffic System Performance: Prototype Field Implementation." The focus of this research included the following: significant expansion and enhancement of the ILD-based vehicle reidentification system at a major signalized intersection in Irvine, California to address reidentification of turning vehicles in addition to through vehicles; derivation of improved estimates of fundamental real-time traffic parameters such as speed, volume and vehicle class from single loop detector inductive signatures; development of a new technique for on-line real-time intersection level of service estimation; implementation of a capability for communicating real-time traffic performance data to operators in the City of Irvine Transportation Management Center (TMC); development of a prototype real-time web-site for internet-based access to performance data from the study intersection in Irvine (and other sites in the future); initial testing of a new state-of-the-art detector card (the IST-222, from IST, Inc.); and an initial study of video image processing for future detector data fusion of video and loop signature data.

This study implemented a real-time traffic surveillance system based on vehicle reidentification technology utilizing vehicle inductive signatures. The developed system has been operated at the intersection of Alton Parkway and Irvine Center Drive in the City of Irvine, California. Although the signalized intersection problem is more complex and challenging than that of a freeway mainline, good real-time traffic performance results have been obtained to date even though signal phase information and some loops were not yet available at the study site. The present system yields valuable real-time traffic information including section travel time obtained by matching vehicle signatures from upstream and downstream detector stations. Such travel times have been identified by Caltrans as particularly important for assessing traffic system performance. In addition, the real-time level of service procedures developed in this study are readily transferable to other signalized intersections, and the derived LOS criteria for through and turning vehicles are potentially of considerable value to operating agencies interested in real-time congestion monitoring, control, system evaluation, and provision of real-time traveler information.

This study has also shown that the use of inductive vehicle signatures offers significant advantages for single loop estimation of various real-time traffic flow characteristics, including vehicle speeds and vehicle classification. This enables the loop-signature-based vehicle reidentification approach developed by the authors to be widely applied in practice, and not limited by the existence of double loops.

The direct estimation of real-time traffic performance data via the developed traffic surveillance system and its availability over the internet will facilitate implementation of a variety of new Advanced Traffic Management and Information System (ATMIS) strategies in California (and elsewhere).

9.2 FUTURE RESEARCH

As discussed in Chapter 1, the multi-year research effort of which Phase I (this report) represents the first year, consists of three major components, based on fully instrumented signalized intersection and freeway sites in the California Advanced Transportation Management Systems Testbed in Southern California. With respect to Phase I, the very encouraging results obtained to date for signalized intersection application of the vehicle reidentification approach suggest that further development and improvement of the vehicle reidentification algorithms for this application would clearly be of value.

The second component of the research is a field investigation of several emerging and advanced freeway detector technologies developed by the PATH program, including laser and/or video detectors, and a particularly promising new detector named the Embedded Differential Inductance Scanning (EDIS) detector. The EDIS detector has a resolution several orders of magnitude greater than regular ILD's and addresses many of the shortcomings of ILD's.

The third component involves an investigation of the fusion of the various advanced detection systems that have been developed by the PATH program (as well as the EDIS detector) for the purpose of vehicle reidentification (or tracking vehicles from one site to another). Until now, each advanced surveillance system has been researched independently and vehicle reidentification has been studied using feature vectors from a single type of detector.